Precision microwave spectroscopy of the ground-state hyperfine splitting in muonium atom

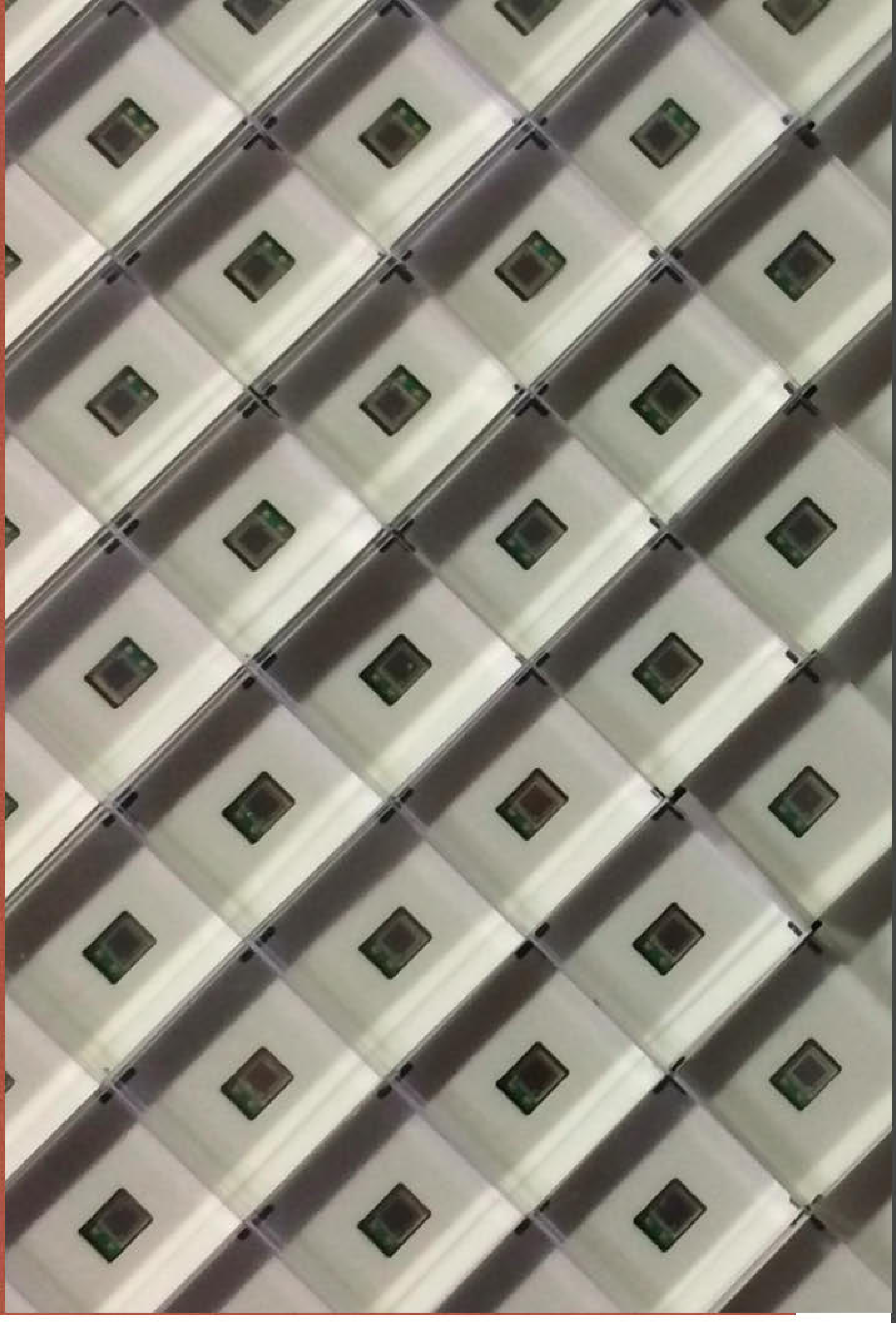

Sohtaro Kanda / 神田 聡太郎

sohtaro.kanda@riken.jp

2019/11/26

Hydrogen Atom Spectroscopy

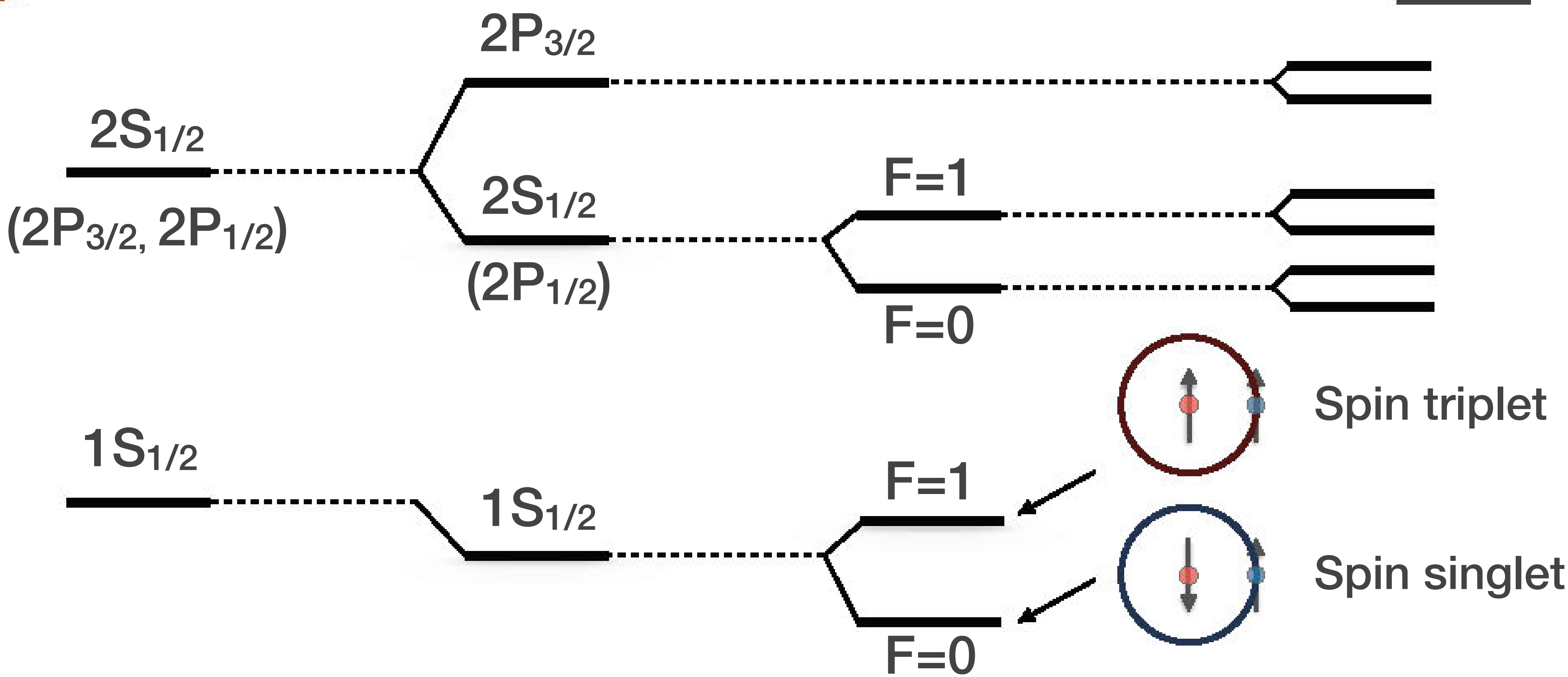

Lyman series (1906)
Bohr model (1913)

Hyperfine structure (1881)
Nuclear magnetic moment (1924)

Fine structure (1887)
Sommerfelt-Bohr model (1916)

Lamb shift (1947)
QED (1949)

- Spectroscopy of hydrogen atoms has led to the development of quantum mechanics and quantum field theory.

HFS of Hydrogen-like Atoms

- Hydrogen
- 1420 MHz
- Atomic hydrogen maser

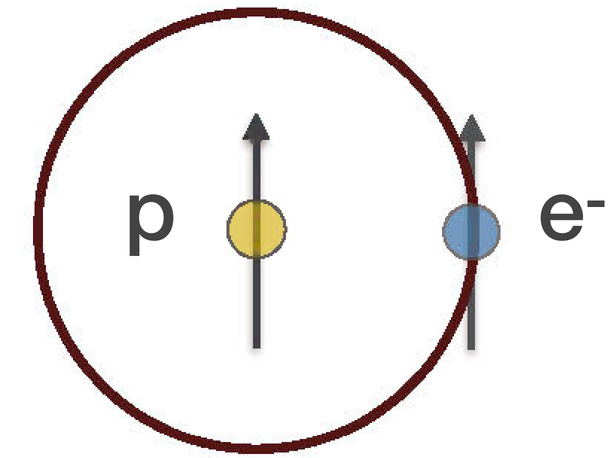

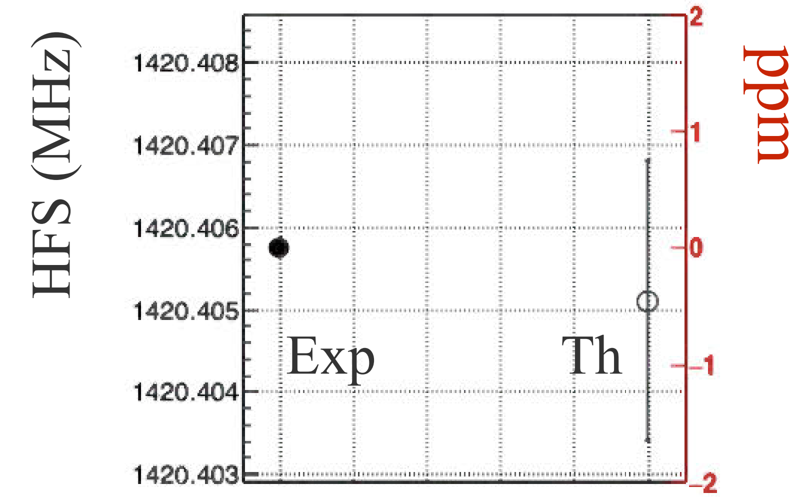

- Muonium
- 4464 MHz
- Decay positron asymmetry

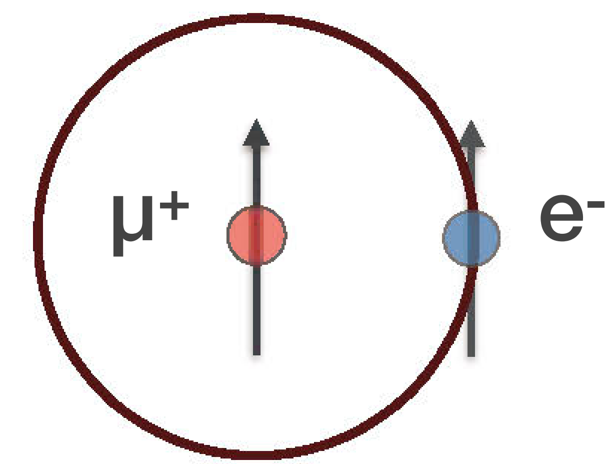

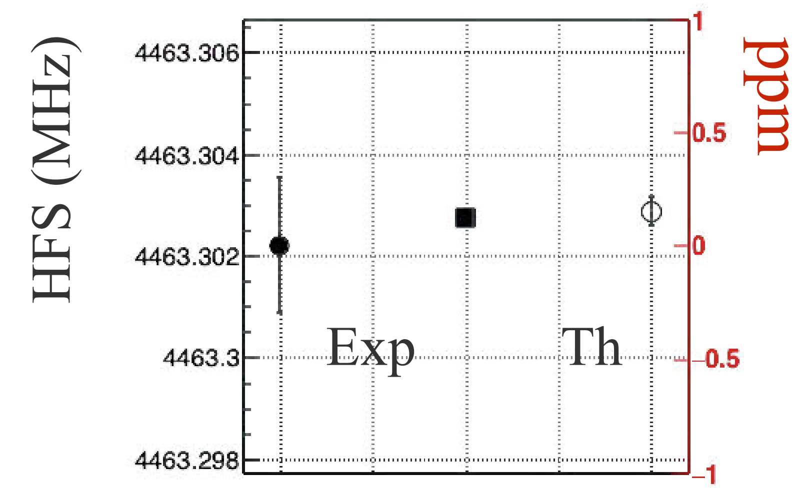

- Positronium
- 203 GHz
- Annihilation gamma rays

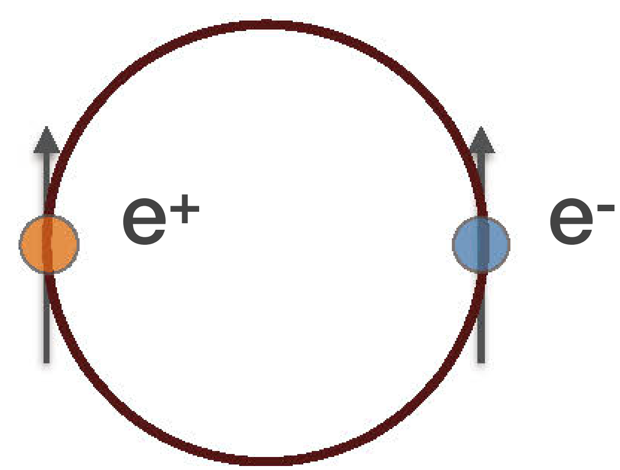

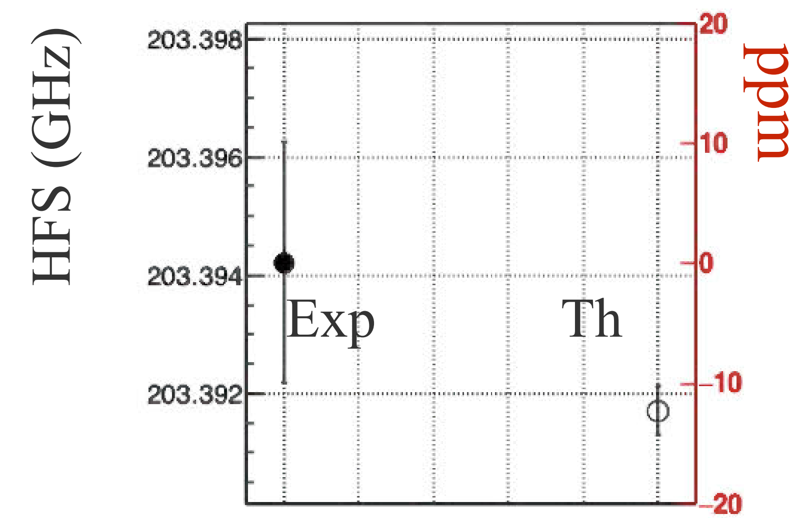

- Muonium provides the most precise theory/experiment comparison.

Precision Test of Bound-State QED

- **Theoretical prediction of muonium HFS**

$$\Delta\nu_{\mathrm{Mu}} = 4\ 463\ 302\ 868(271)\ \mathrm{Hz}$$

- **Contributions from each sector**

$$\Delta\nu_{\mathrm{Mu\ (QED)}} = 4\ 463\ 302\ 700\ (271)\ \mathrm{Hz}$$

$$\Delta\nu_{\mathrm{Mu\ (QCD)}} = 232.7\ (1.4)\ \mathrm{Hz}$$

$$\Delta\nu_{\mathrm{Mu\ (EW)}} = \text{-}65\ \mathrm{Hz}$$

- **Theoretical uncertainty**

Term	Contribution (Hz)
Radiative correction	5
Recoil correction	64
Radiative recoil correction	55
Hadronic correction	1.4
Total	85

- **Dominant uncertainties are arising from errors in physical constants (fine structure constant, Rydberg constant, and muon mass).**

D. Nomura and T. Teubner, Nuclear Physics B 867 (2013) 236-243.

Muon-to-Electron Mass Ratio

- **By comparing the theoretical expression and experimental result of the muonium HFS, the muon-to-electron mass ratio can be extracted.**

$$\nu_{\text{theory}} = \frac{16}{3}\alpha^2 c R_\infty \frac{m_e}{m_\mu}\left[1 + \frac{m_e}{m_\mu}\right]^{-3} + \delta(\alpha,\ m_e/m_\mu)$$

- **The muon-to-electron mass ratio is one of the necessities to the experimental determination of the muon anomalous magnetic moment (muon *g*-2).**

$$a_\mu(\text{Exp.}) = 11\ 659\ 208.9(6.3)$$
$$a_\mu(\text{Theory}) = 11\ 659\ 181.8(4.9)$$

$$a_\mu = \frac{g_e}{2}\frac{\omega_a}{\omega_p}\frac{\mu_p}{\mu_e}\frac{m_\mu}{m_e}$$

P. J. Mohr, D. B. Newell, and B. N. Taylor, "CODATA2014", Rev. Mod. Phys. 88, 035009 (2016).

G.W. Bennett *et al.*, Phys. Rev. D73, 072003 (2006). K. Hagiwara *et al.*, JPHGB G38, 085003 (2011).

Test of Lorentz Invariance

- **Sidereal oscillation of the transition frequency means Lorentz invariance violation.**

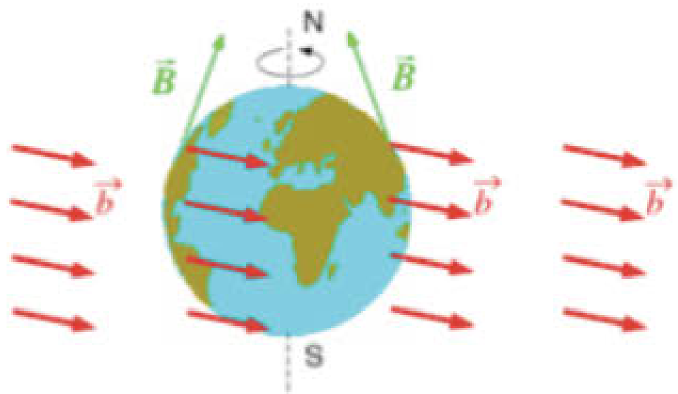

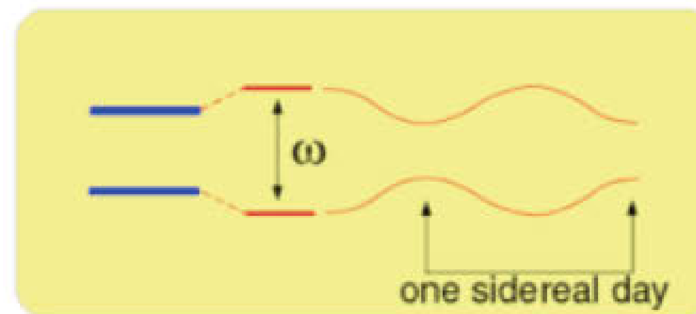

R. Bluhm, V.A. Kostelecký, and C. Da Lane, Phys. Rev. Lett. 84, 1098 (2000).

- **Limits on the model parameters from the muonium HFS.**

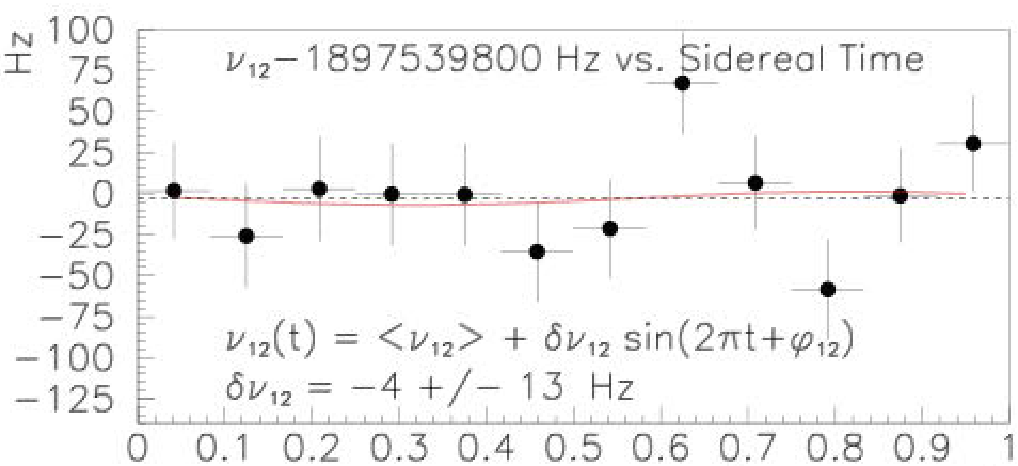

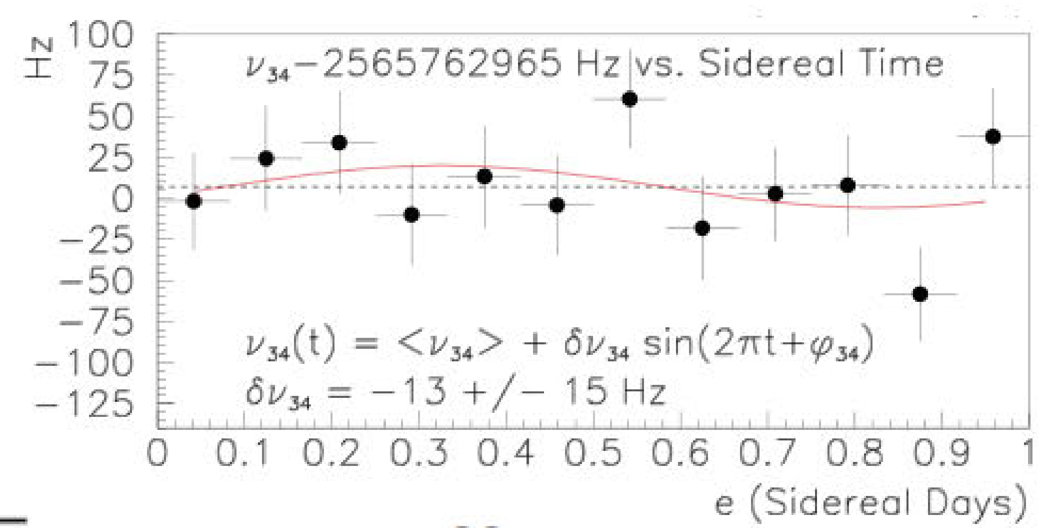

$$|\sin\chi|\sqrt{(\tilde{b}_X^{\mu})^2 + (\tilde{b}_Y^{\mu})^2} \lesssim 2\times 10^{-22}\ \mathrm{GeV}$$

V.W. Hughes *et al*., Phys.Rev.Lett.87, 111804 (2001).

Searches for Exotics

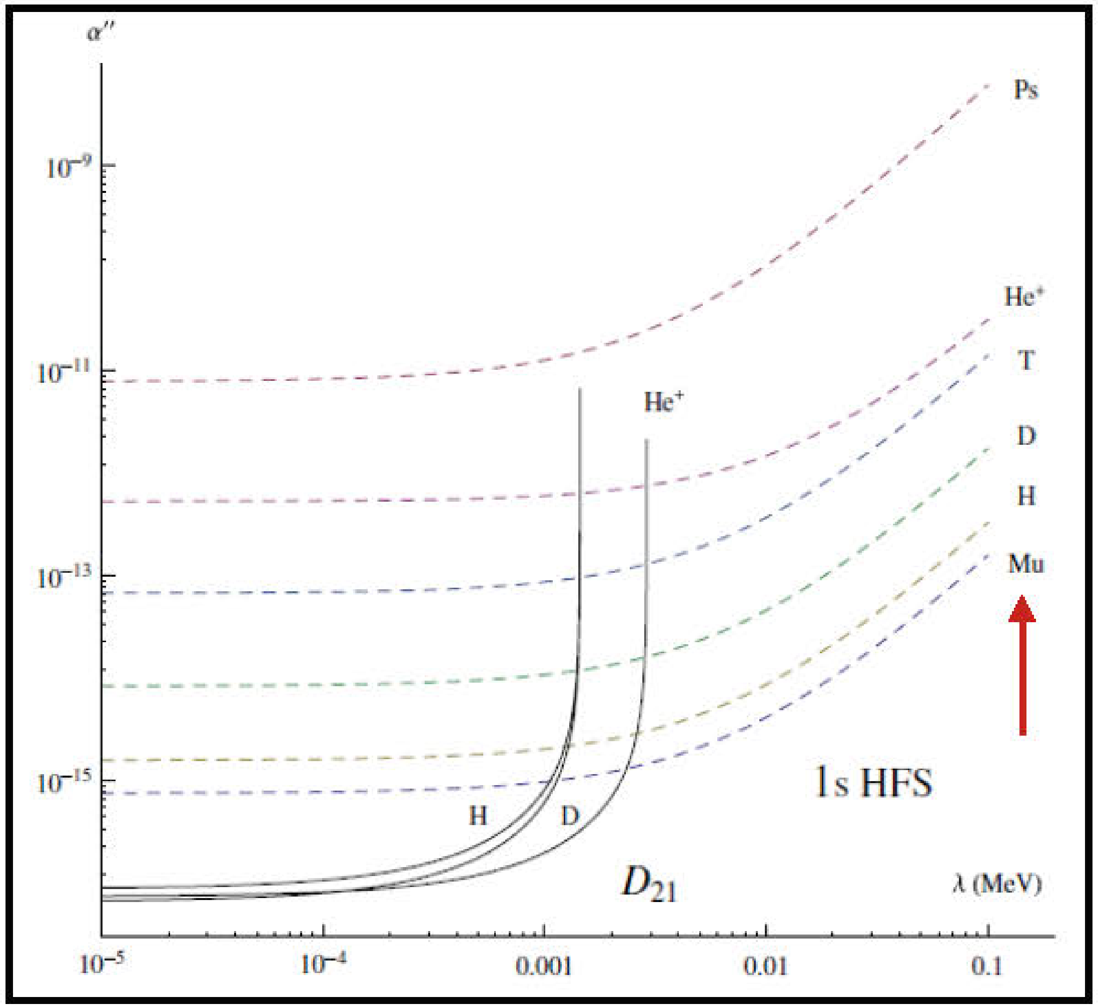

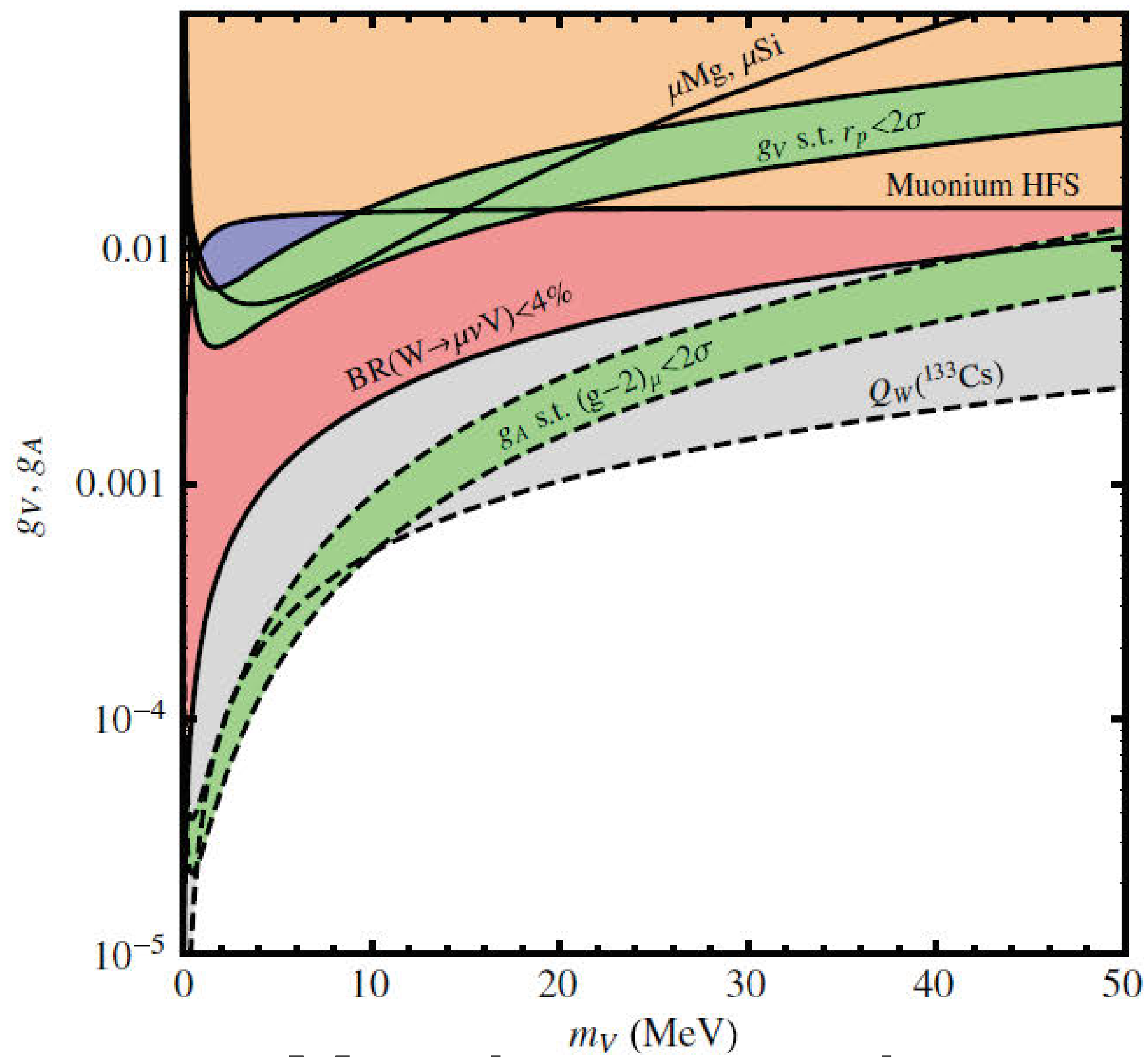

Light pseudo-vector boson

S. G. Karshenboim, PRL 104, 220406 (2010).

Massive vector boson

S. G. Karshenboim, PRD 90, 073004 (2014).

- **Muonium HFS constraints "dark" force carriers.**
- **Test of lepton universality via a search for muon-specific force.**

Direct and Indirect Measurements

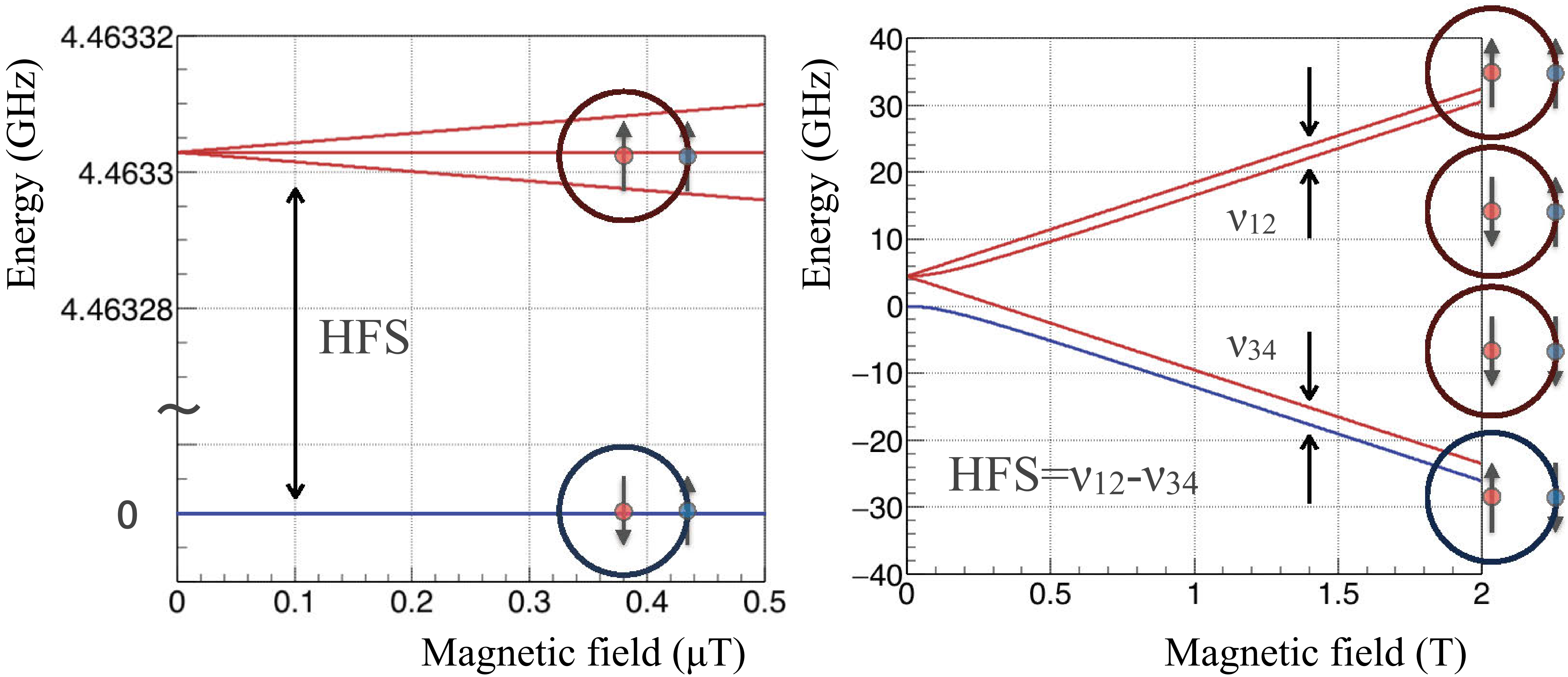

- Two independent methods for the hyperfine splitting measurement
  - <u>Direct measurement at "zero" magnetic field (ZF, in progress).</u>
  - Indirect measurement in a high magnetic field (HF, in preparation).
- Our goal is ten-fold of improvements in both ZF and HF experiments.

Parity Violating Muon Decay

- **Muon decay is mediated by the weak boson.**
- **Muon spin and emission angle of decay positron correlate.**
- **More positrons are emitted in parallel with the muon spin direction.**
- **By measuring the angular asymmetry of the decay positron, the muon spin can be obtained as an ensemble average.**

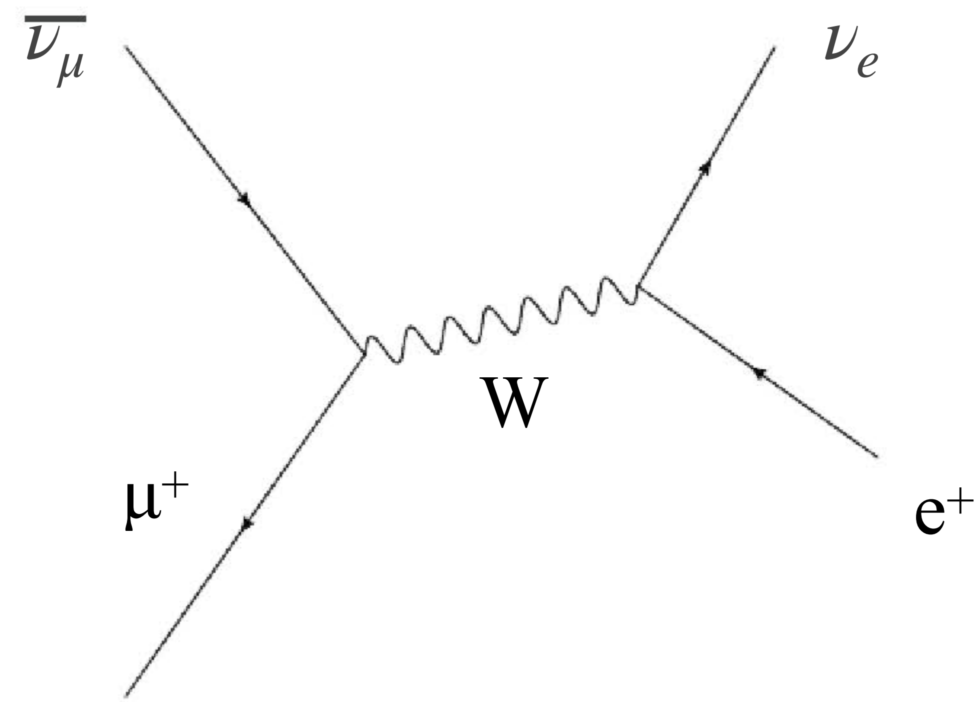

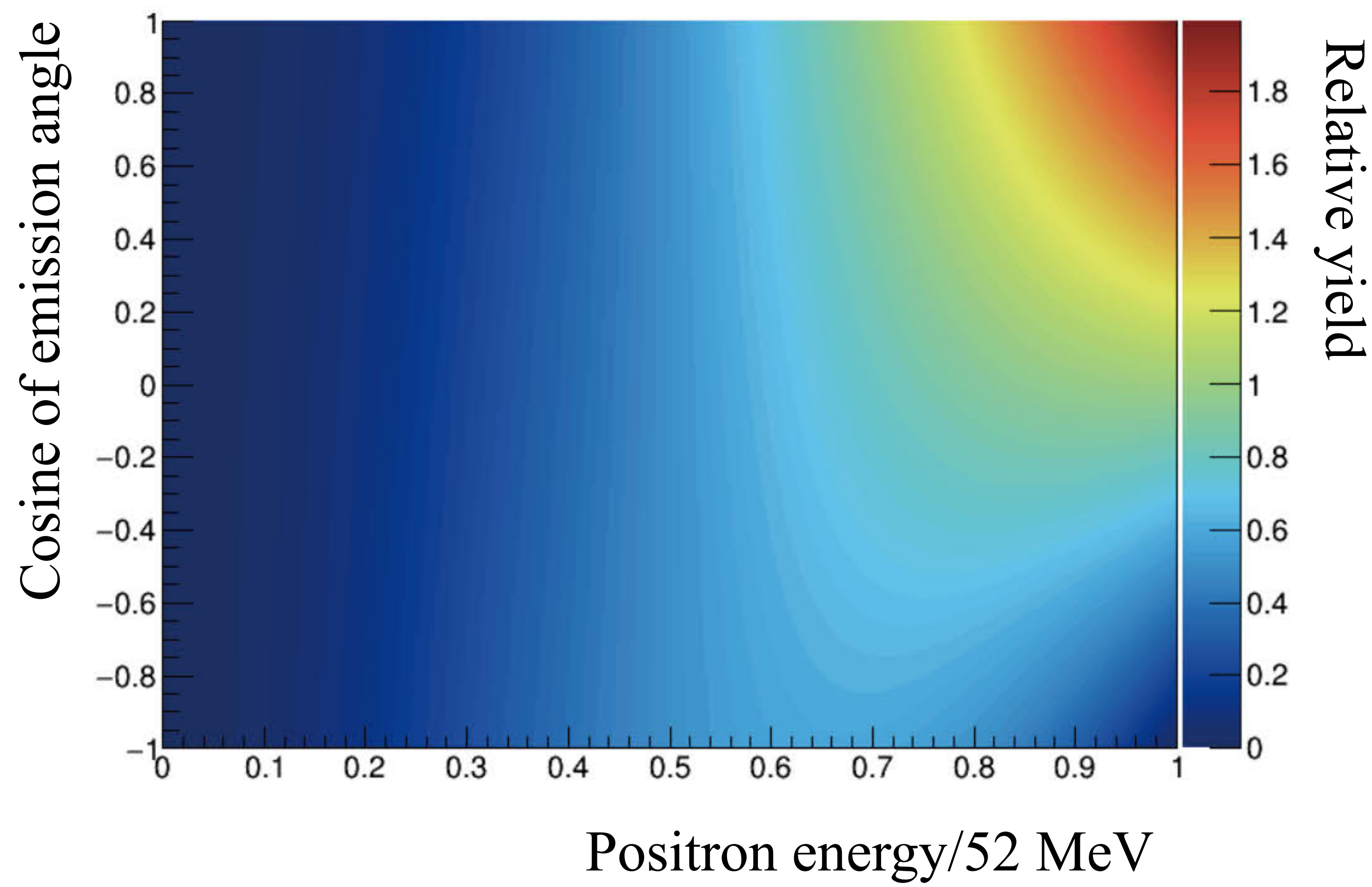

Rabi Oscillation

- **Muon spin flips after the hyperfine transition induced by the microwave irradiation.**
- **State population of muonium changes as a function of muonium age.**
- **Muon spin polarization oscillates with the Rabi frequency.**
- **Typical oscillation frequency is on the order of MHz.**
- **A time-window of several μs is required to observe the signal.**

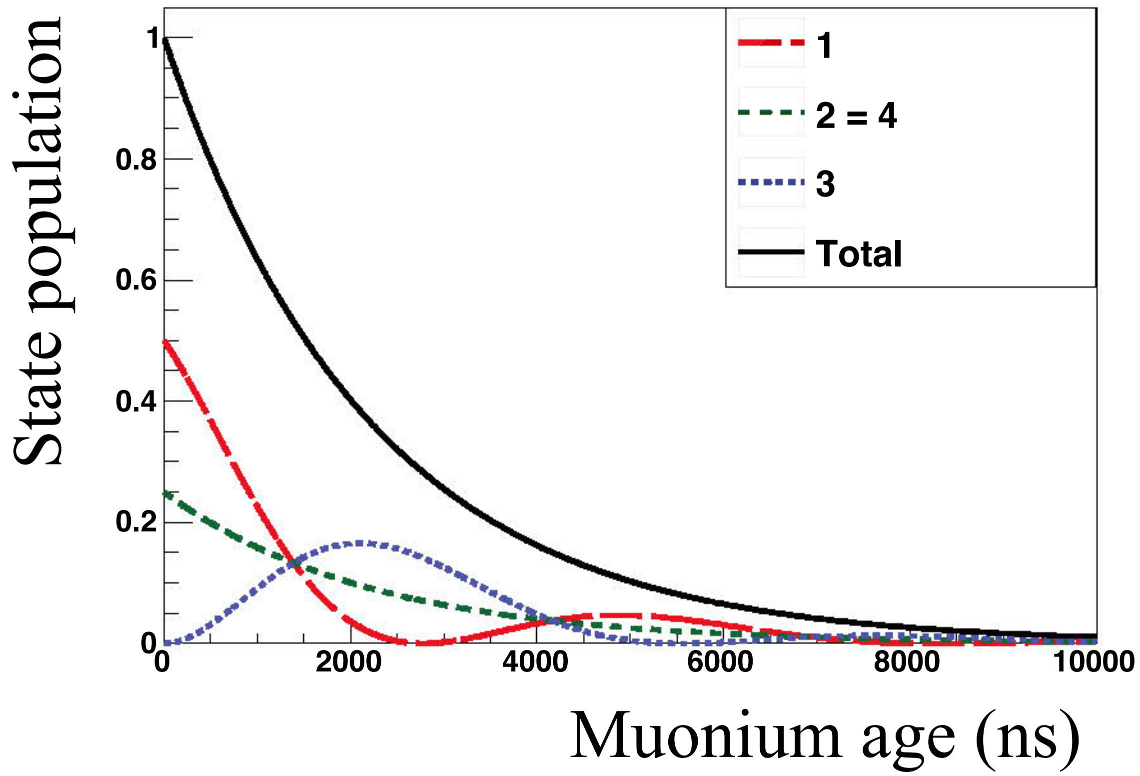

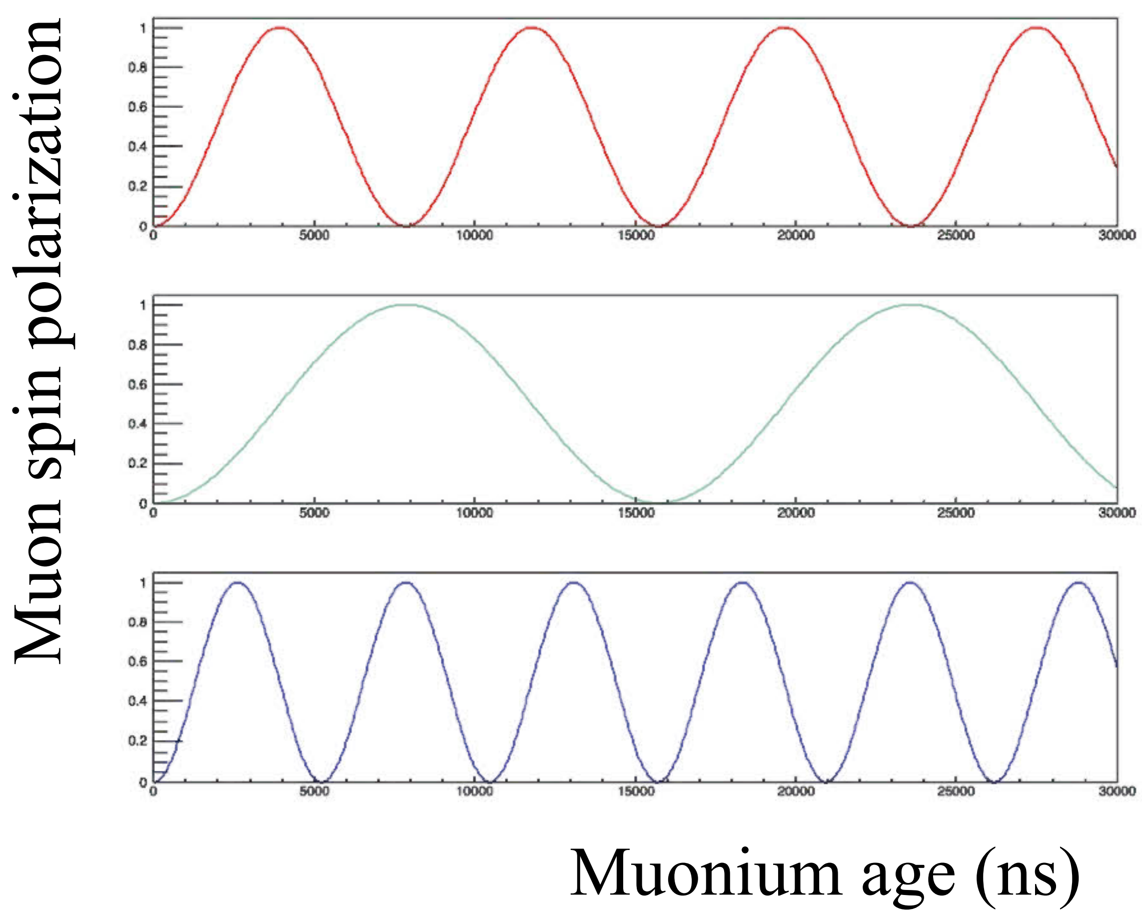

Precursor Experiments at LAMPF

- An experiment at Los Alamos National Laboratory.
- A continuous muon beam irradiates the krypton gas target.
- The muon beam intensity was limited to avoid muon pileup.
- Statistical uncertainty was 1.4 kHz with 600 hours of measurement.
- No quantitive estimation of the systematic uncertainties.
- High-intensity pulsed muon beam is a key for improvement.

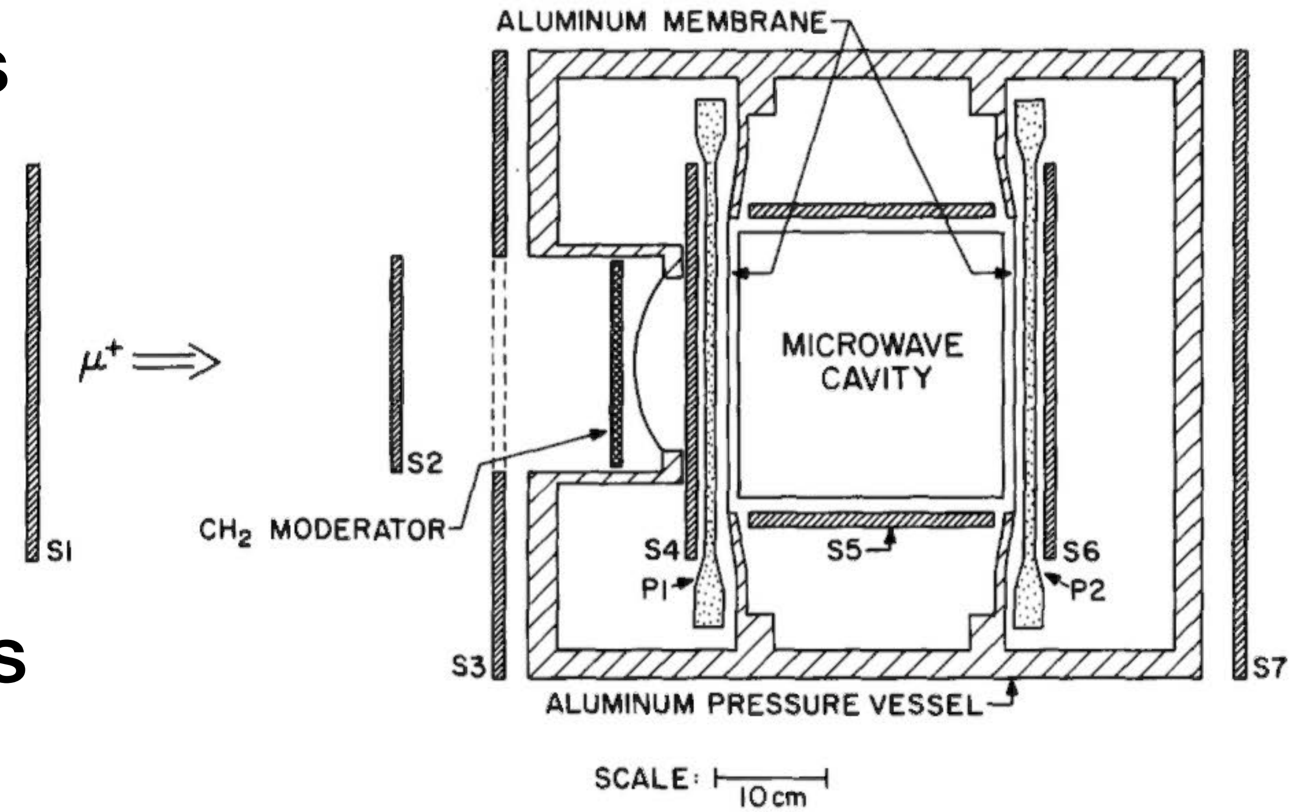

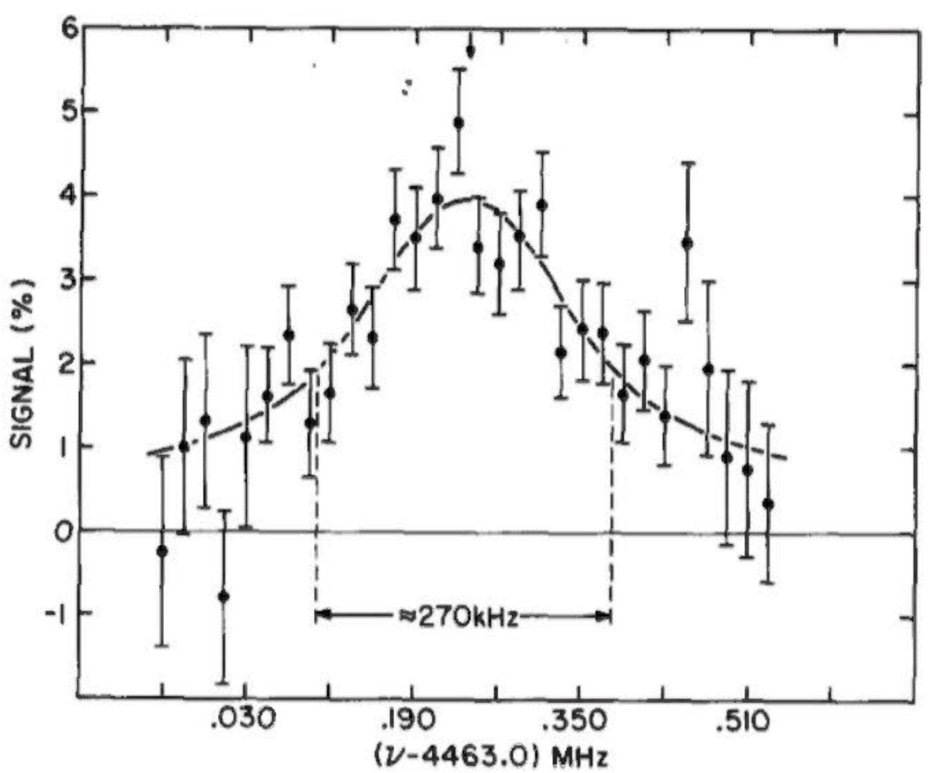

D.E. Casperson *et al.*, Phys. Lett. 59B, 4 (1975).

MuSEUM Experiment

- Muonium Spectroscopy Experiment Using Microwave
  - Zero field: Demonstration at existing beamline.
  - High field: Highest precision experiment at dedicated beamline under construction.

	2011	2013	2015	2017	2019
ZF			R&D	1st ZF, 2nd ZF	3rd ZF, 4th ZF
HF	Proposal Submitted	R&D	R&D	New Beamline Construction	1st HF?

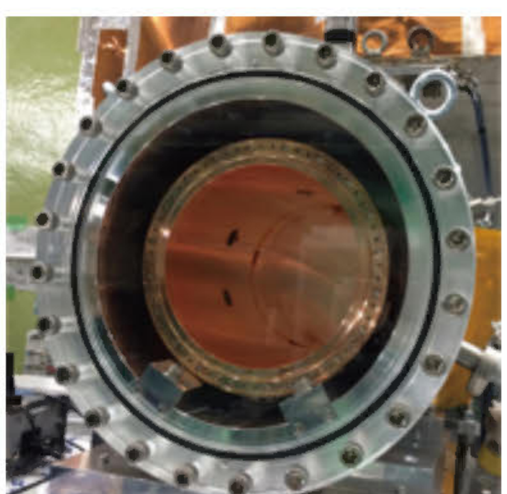

RF Cavity

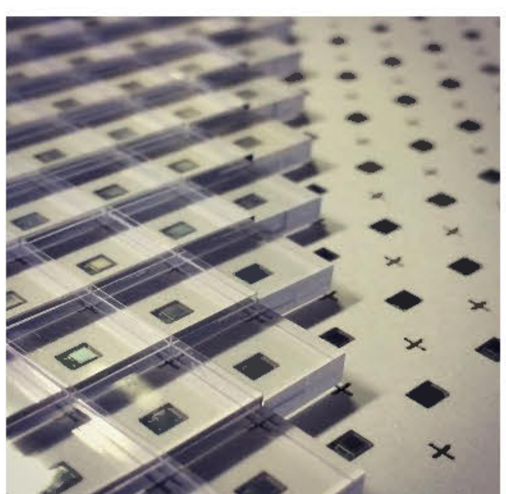

Detector

Magnet

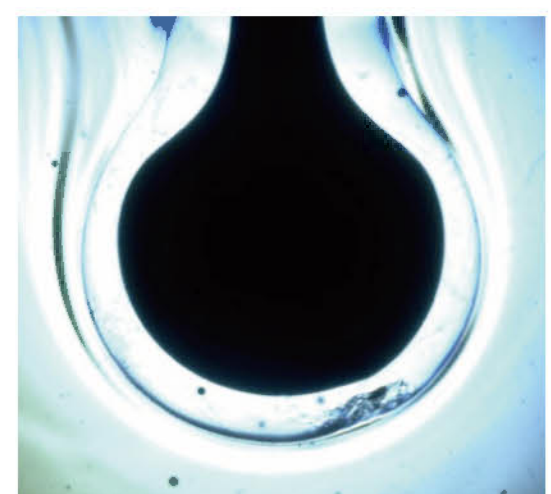

Field probe

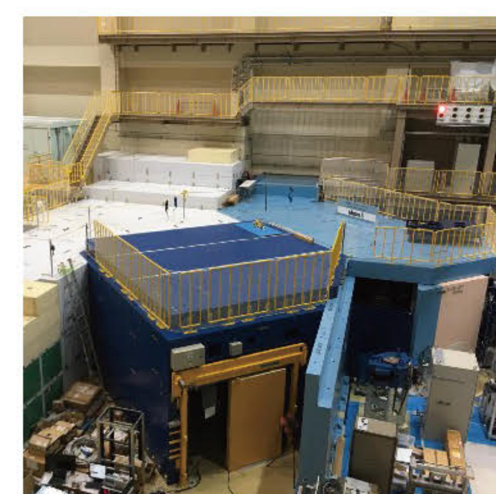

New beamline

J-PARC

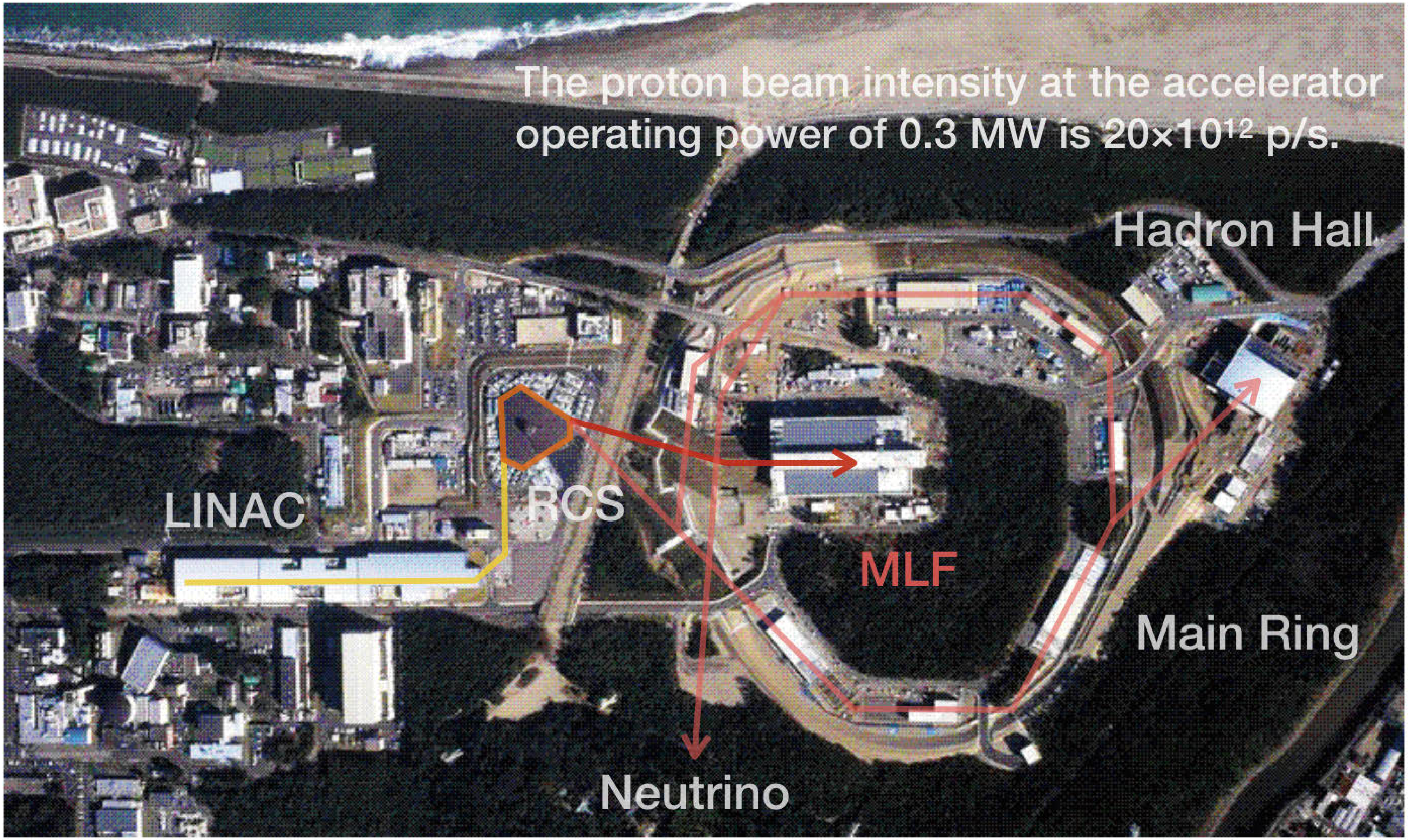

- World's highest intensity proton driver.
- 400 MeV LINAC, 3 GeV RCS, and 30 GeV Main Ring.
- Pulsed proton beam with 25 Hz repetition.

http://j-parc.jp/Acc/ja/layout.html

MLF

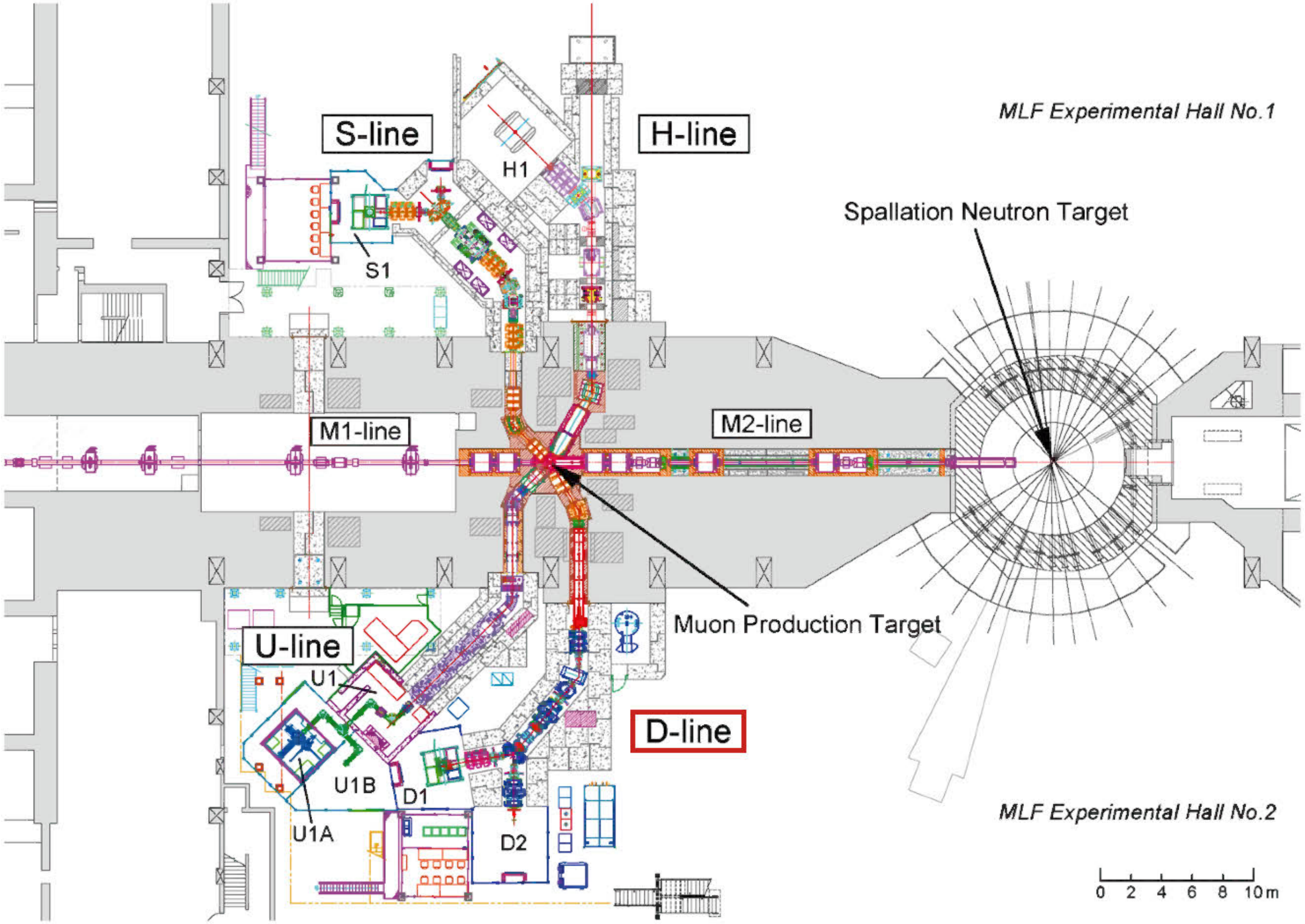

- D (μ+, μ-)
  - Muon spin rotation
  - Muonic X-rays
  - General purpose
- U (μ+)
  - Ultra slow muon
- S (μ+)
  - Muon spin rotation
- H (μ+, μ-)
  - Muonium HFS
  - Muon-to-electron conversion
  - Muon g-2
  - Muon transmission microscope

- **Material and Life Science Facility**
  - **Graphite target for muon production**
  - **Four muon beam lines deliver intense μ^+ and μ^- beams.**
  - **3×10^6 μ^+/s at D-Line (0.3 MW).**

W. Higemoto, *Quantum Beam Sci*. **1** (2017) 11.

MUSE D-Line

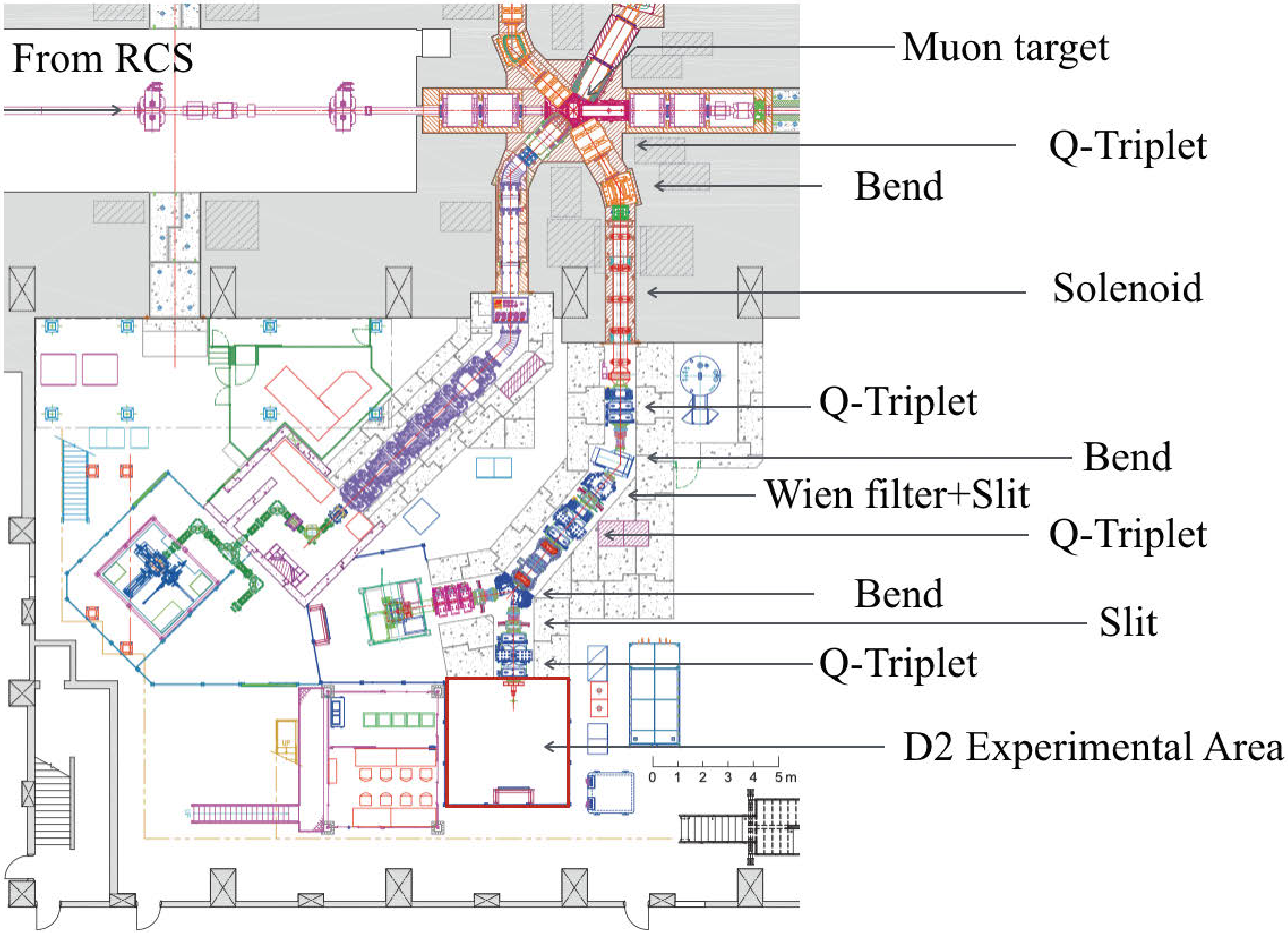

- Multi-purpose beam line for intense, polarized muon beam.
- Positive muons produced on the target surface with the momentum of 27.4 MeV/c are transported.

Experimental Setup

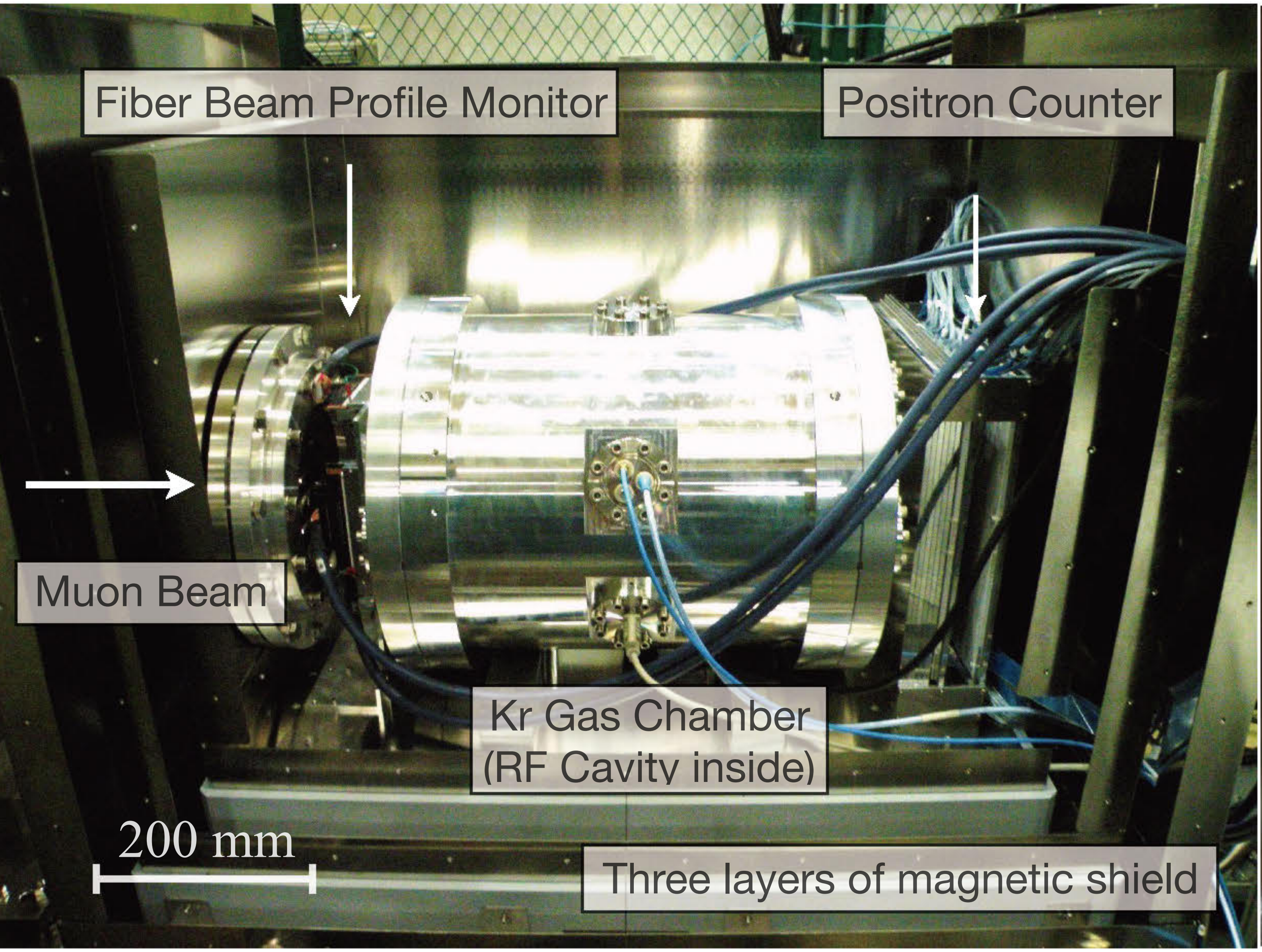

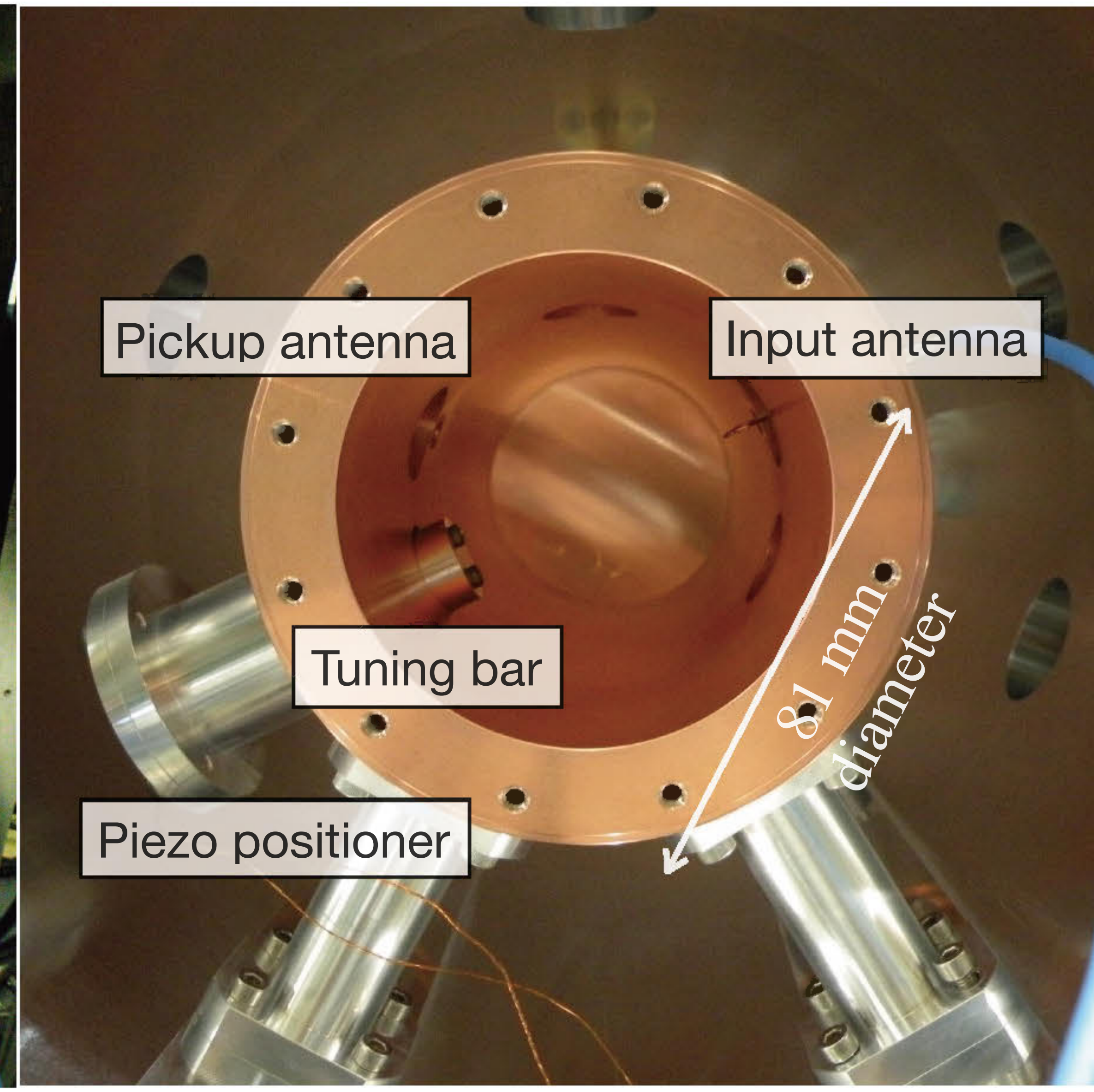

- The apparatus is installed at MLF MUSE D2 experimental area.
- The entire setup was surrounded by a magnetic shield to shield the leakage magnetic field from the beam line and surrounding equipments.

Magnetic Shield

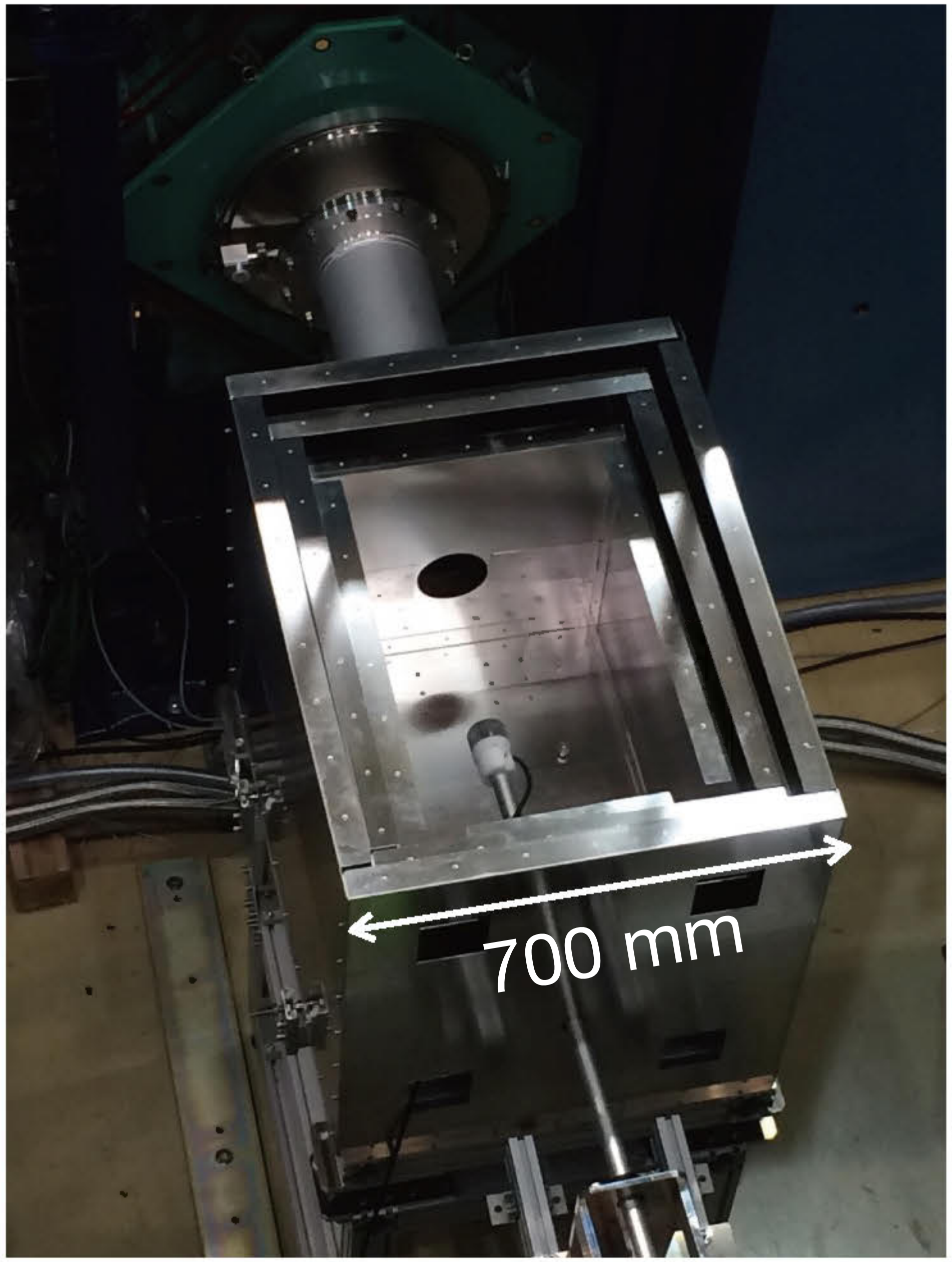

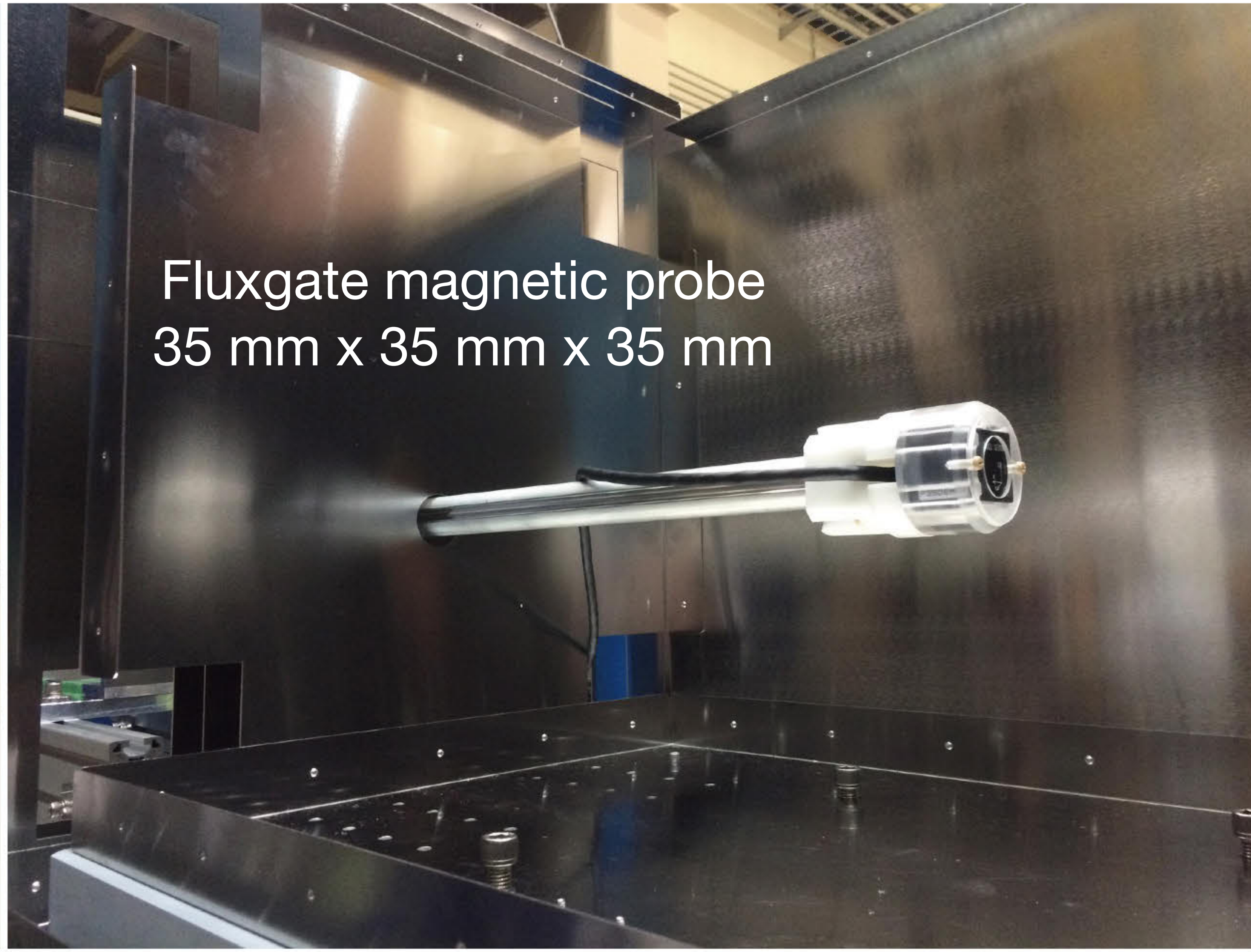

- A three-layer box-type magnetic shield made of an alloy of iron and nickel.
- A magnetic field inside the shield is measured by a fluxgate magneto probe.

S. Kanda, *RIKEN APR* 49, 227 (2017).

Target Gas Chamber

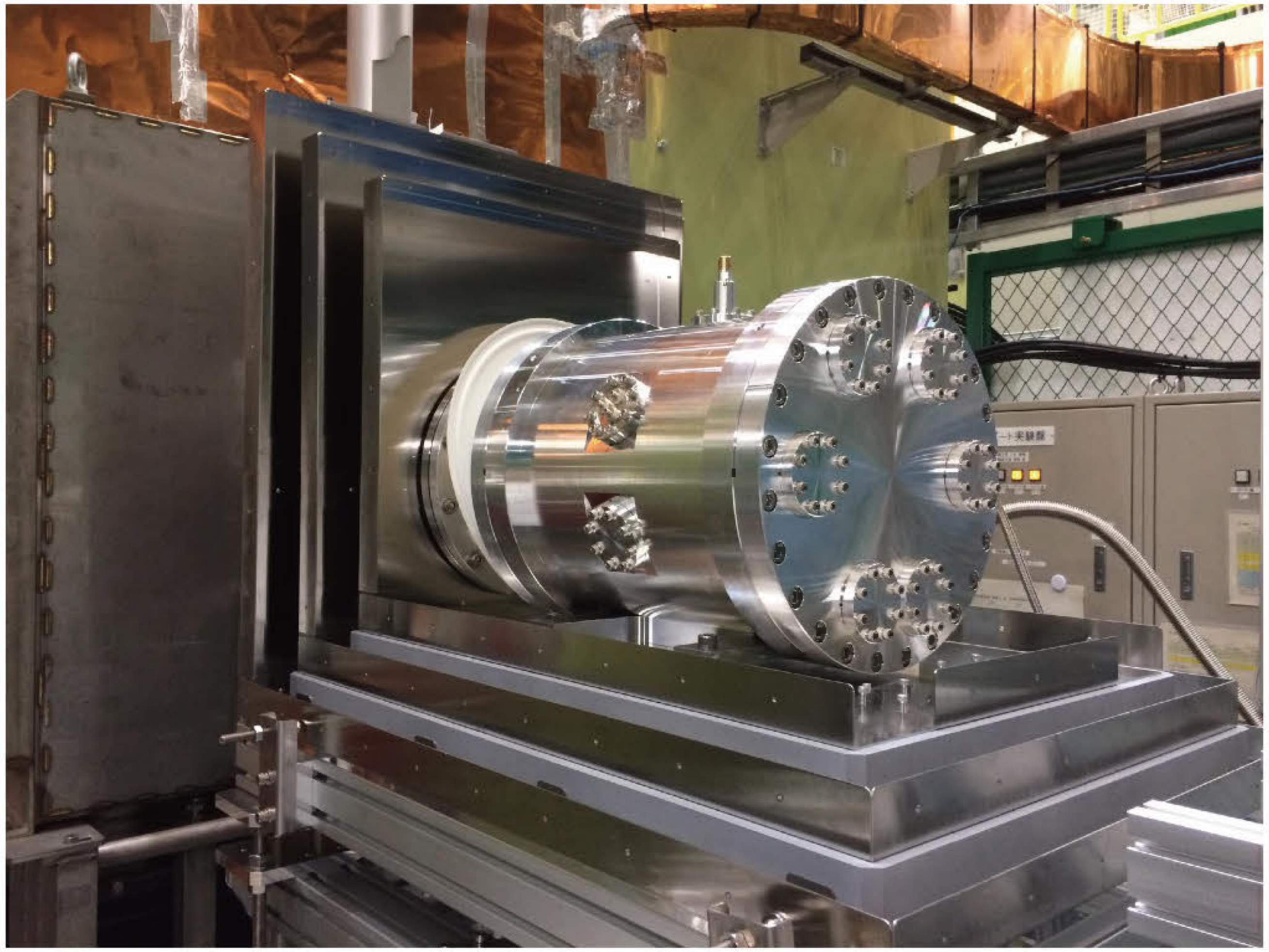

- A cylindrical vessel made of aluminum with a longitudinal length of 450 mm and an inner diameter of 280 mm.
- Target gas is krypton to optimize the energy threshold of muonium formation via electron capture.
- Gas handling panel is developed to fill the chamber with gas, evacuate the chamber, and monitor impurities using a quadrupole mass spectrometer.

Microwave Cavity

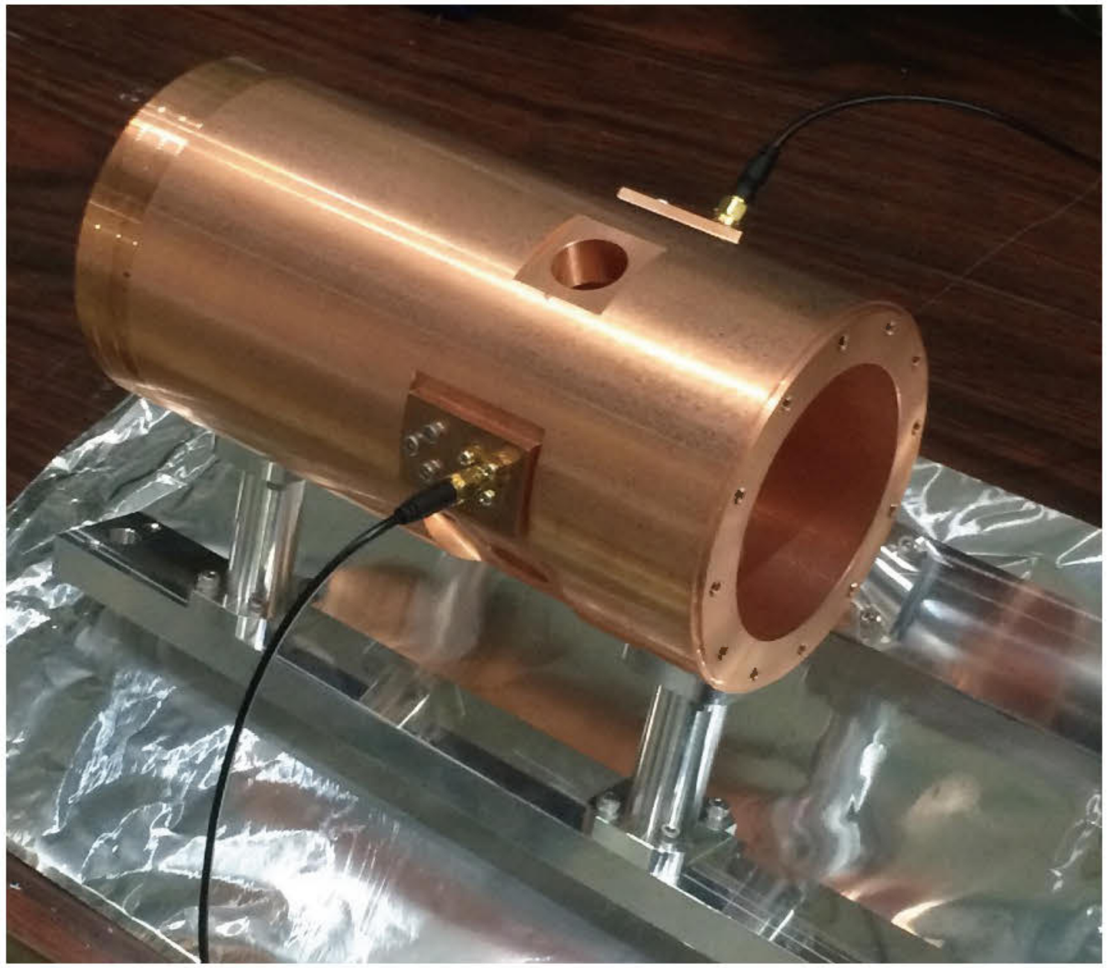

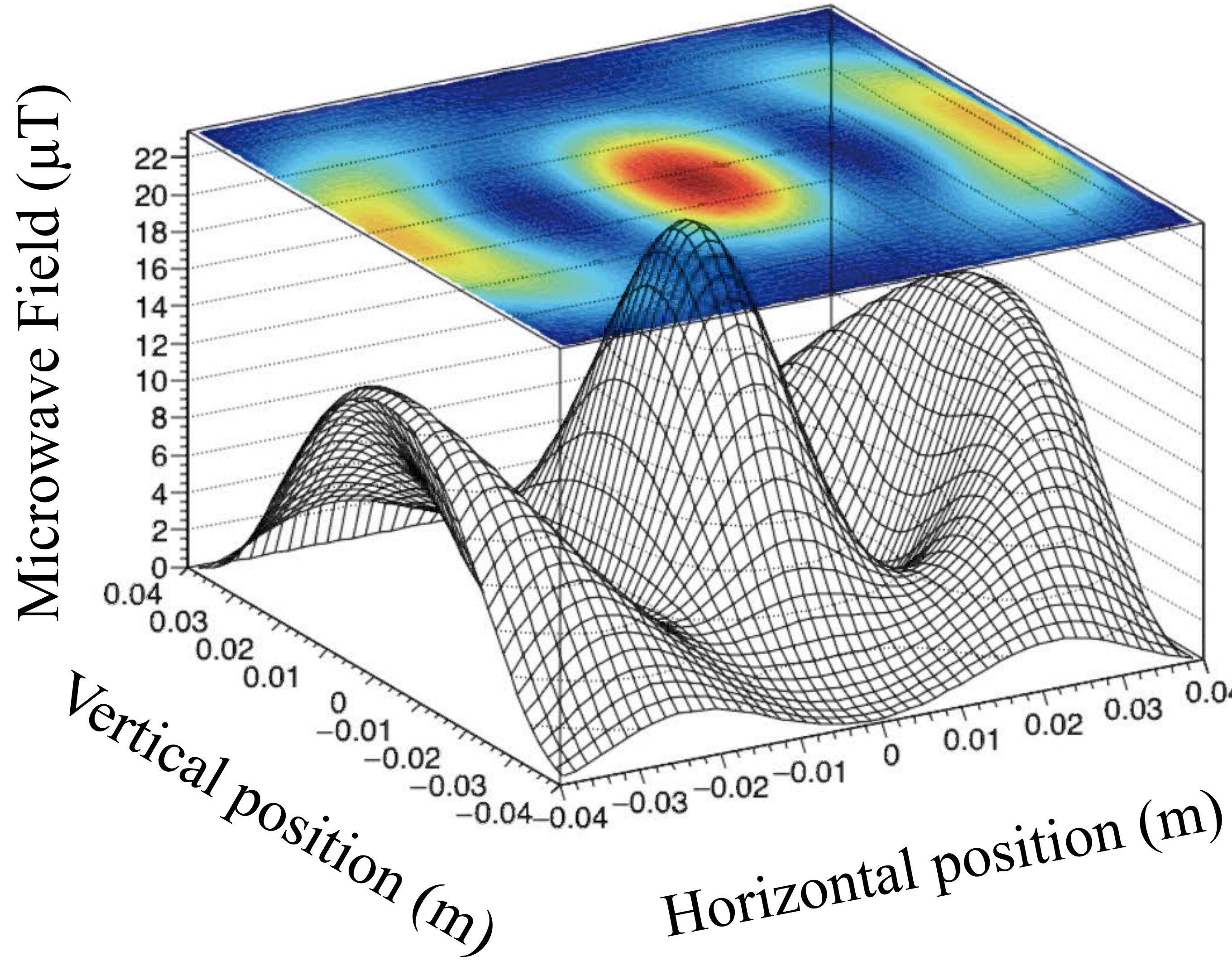

- A cylindrical resonator made of oxygen-free copper with a diameter of 81 mm and an axial length of 230 mm.
- TM110 mode is excited with typical power of 1 W.
- Loop antennas are placed to input and monitor the microwave.
- Resonance frequency is tuned by a piezoelectric positioner.

Cavity Resonance and Quality

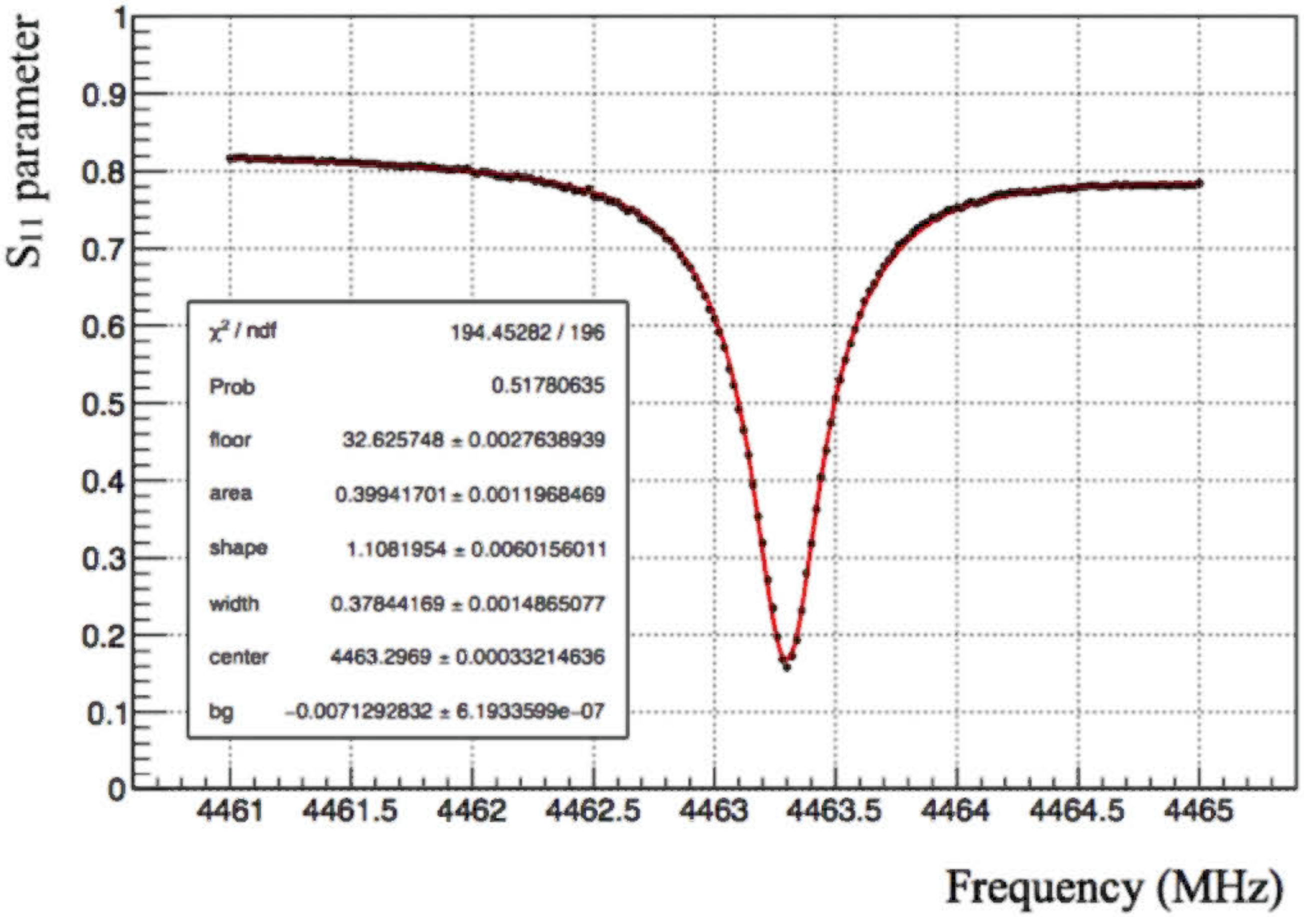

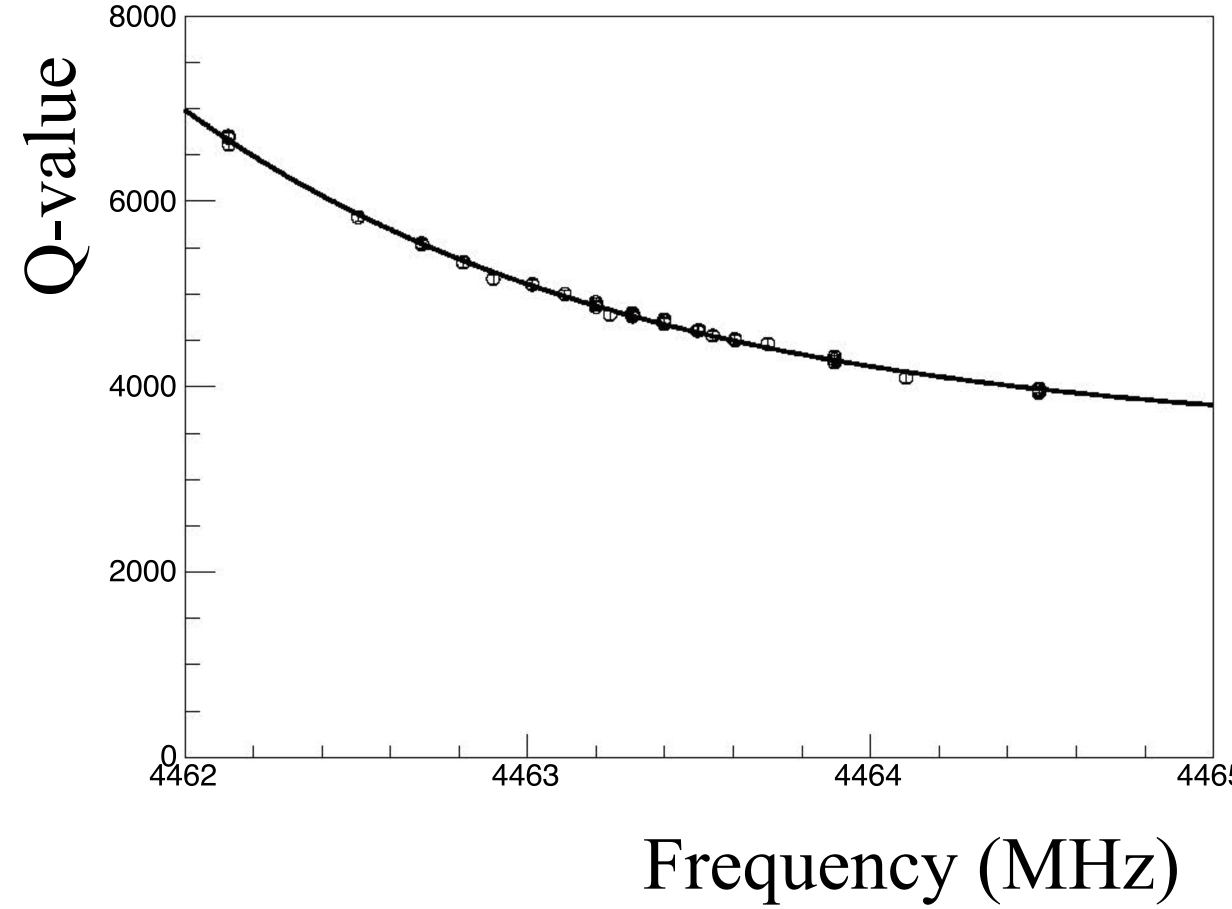

- Resonance of the cavity is observed using a vector network analyzer.
- S11 parameter (reflection) is measured to evaluate the quality value.
- Resonance curve is fitted with a pseudo-Voigt function.
- Typical quality value is 5,000.
- Frequency dependence of the quality value is necessary to analyze a resonance lineshape.

Fiber Beam Profile Monitor

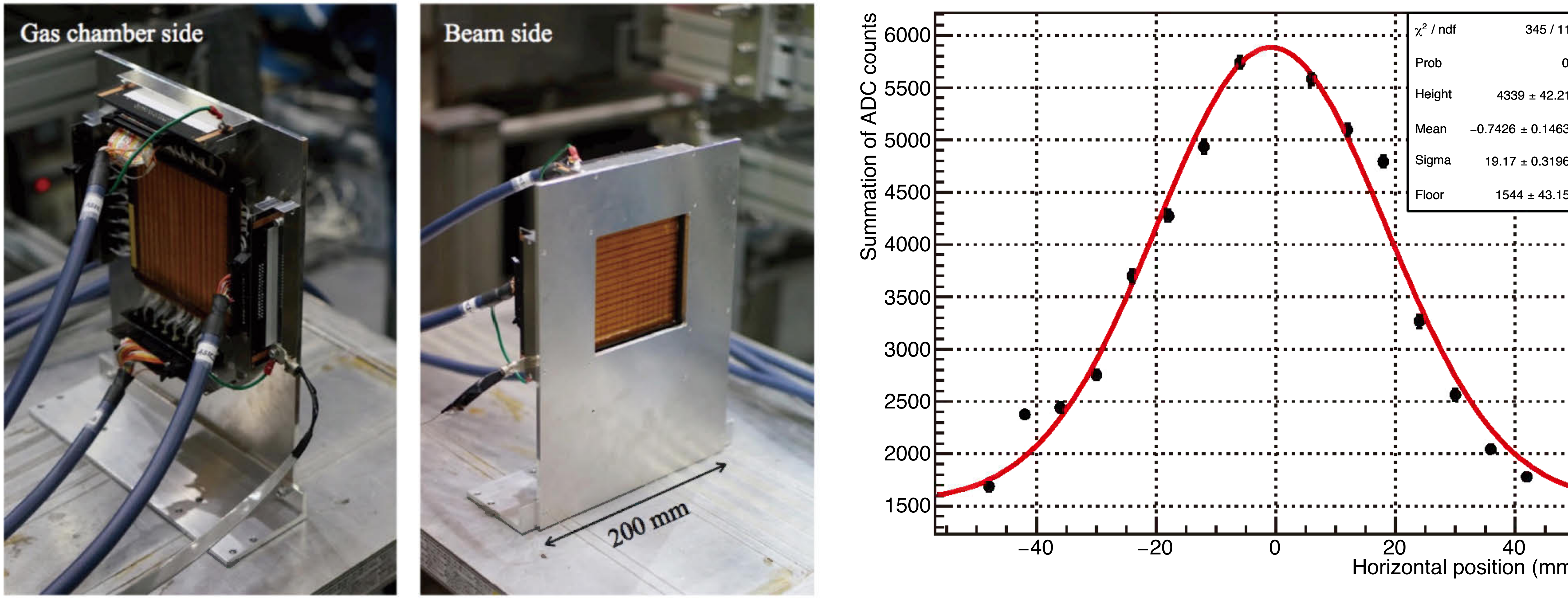

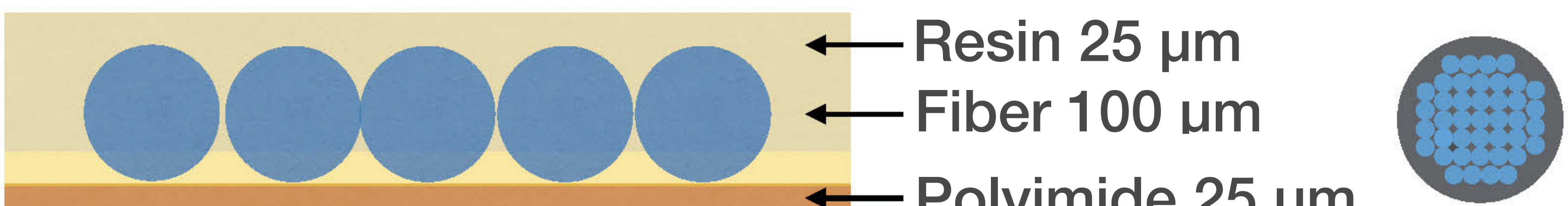

- Cross-configured fiber hodoscope with SiPM readout.
- Online measurement of the beam profile and relative intensity.

S. Kanda, *RIKEN APR* 48, 278 (2016).

Segmented Positron Counter

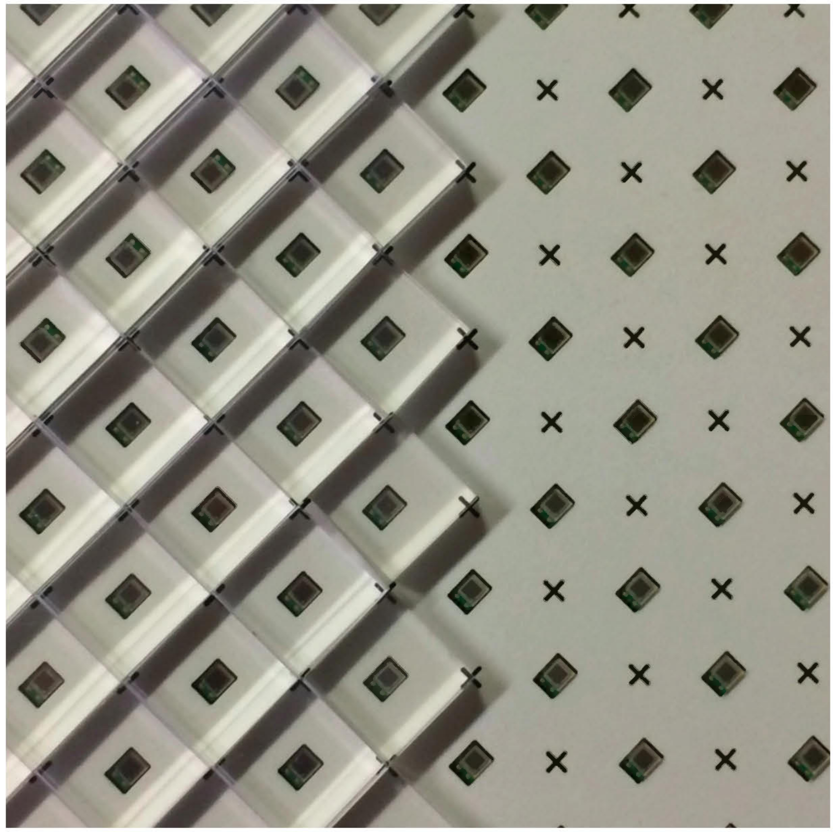

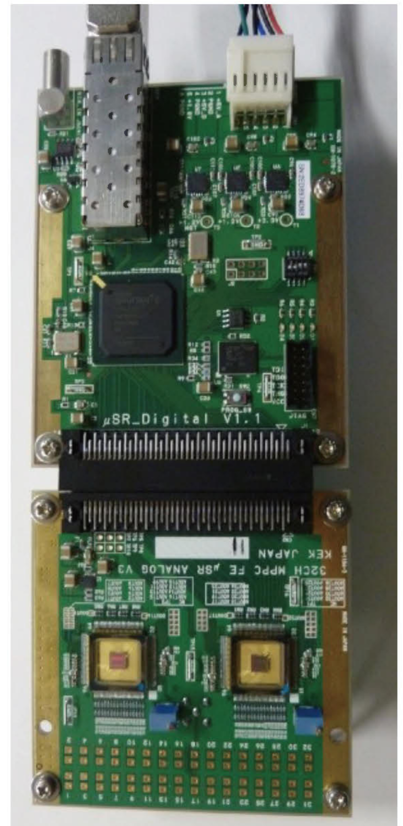

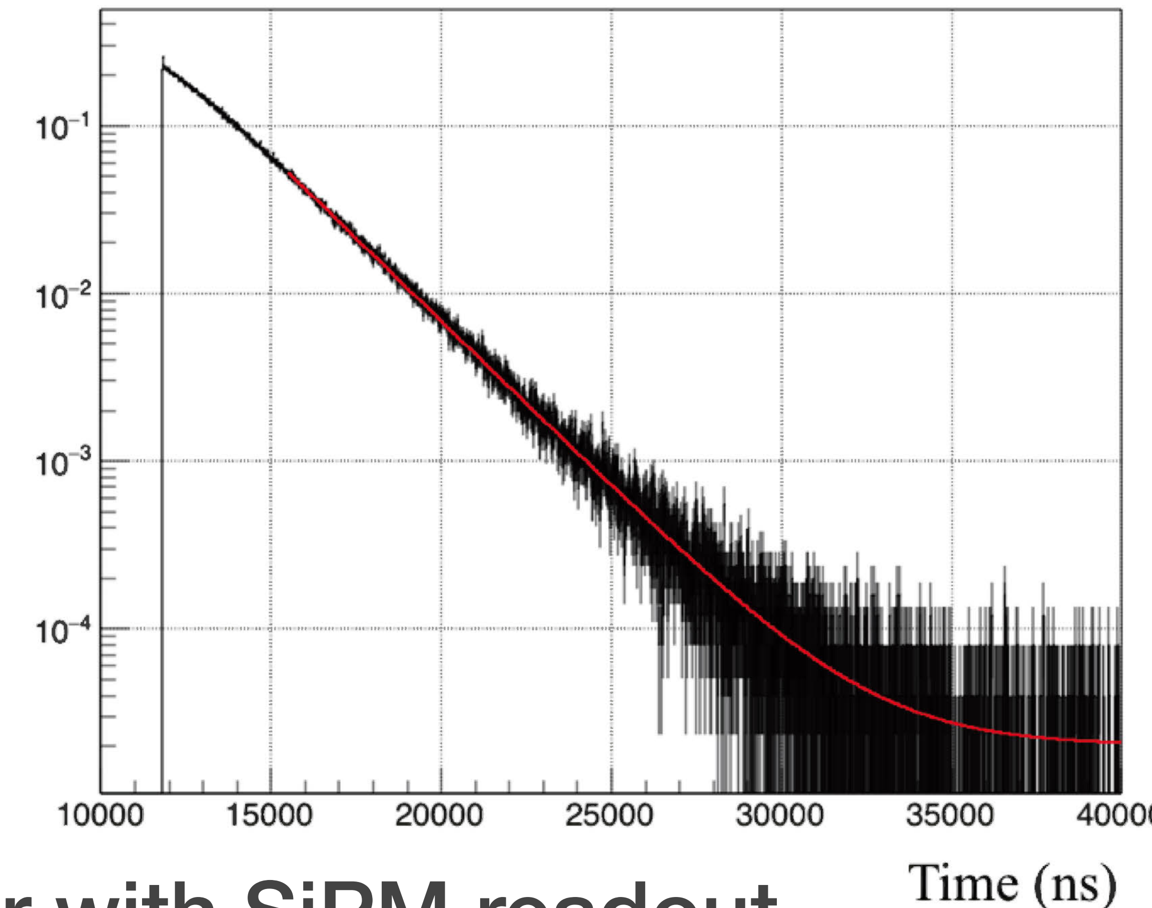

- Segmented scintillation counter with SiPM readout.
  - Unit cell has the dimension of 1 cm x 1 cm x 3 mmt.
  - Reflector film is inserted between scintillators.
  - 240 mm x 240 mm area, 1152 ch. in total.
- Amplifier, shaper, and discriminator are implemented in ASIC.
- FPGA-based multi-hit TDC.

S. Kanda, PoS(PhotoDet16)039 (2016).
K. M. Kojima, S. Kanda et al., J. Phys. Conf. Ser. 551 (2014) 012063.

Segmented Positron Counter

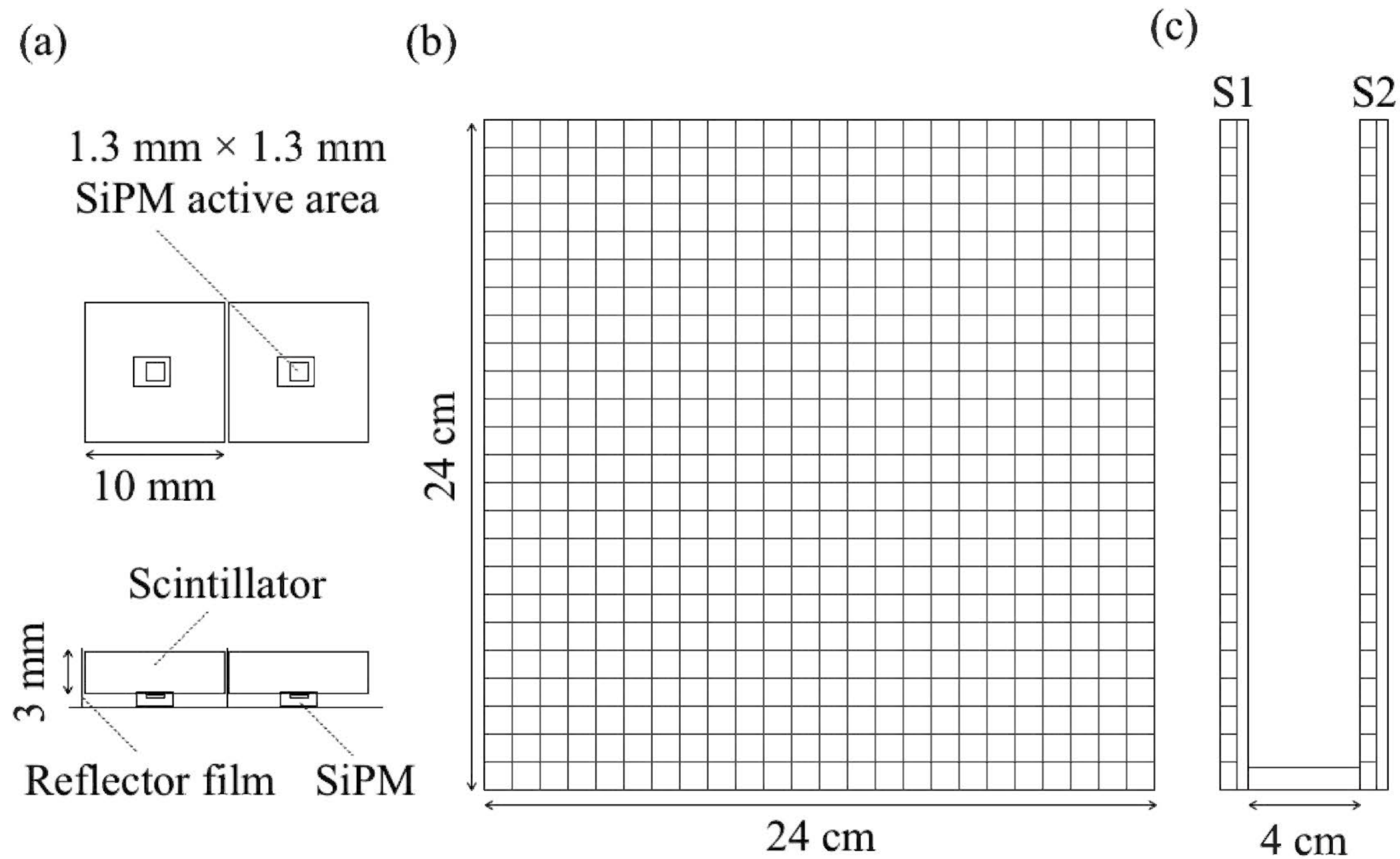

- Two layers of the detector are placed at the interval of 40 mm.
- The decay positron time spectra were analyzed by the coincidence method using two layers of the positron counter.
- Plural simultaneous hits on each layer were merged into a hit cluster to avoid positron over-counting.

Project History 2014-2016

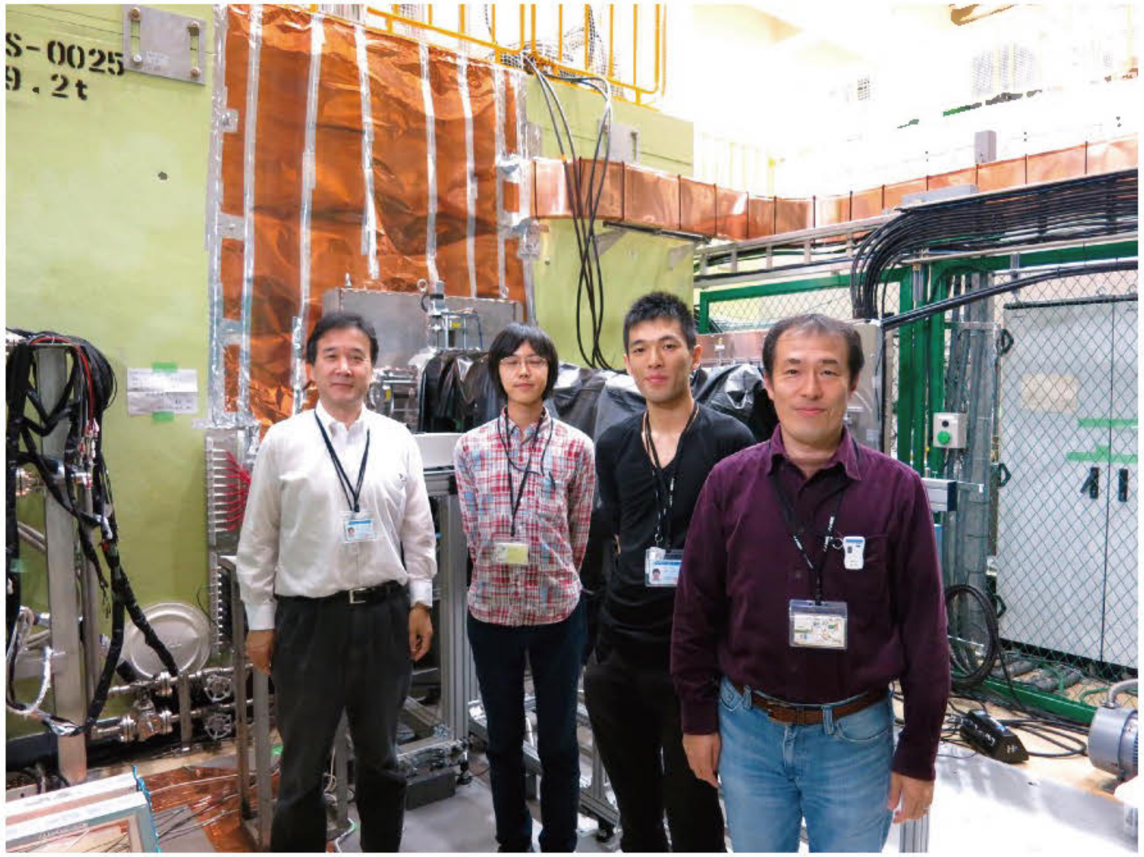

- First trial in 2014.
- No resonance was observed.
- Small signal, severe background.
- No beam delivery in 2015 due to the trouble with the mercury target.

- Second trial in 2016.
- Improvements in the microwave system and suppression of beam-derived background events.
- First observation of the muonium HFS resonance with a pulsed muon beam.

S. Kanda, Proc. of Science, PoS(INPC2016)170 (2017) 1-6.

Project History 2017-2019

- Third experiment in 2017.
- Improvements in background suppression.
- Microwave power dependence was studied.
- Power optimization.
- Today's main topic.

- Forth experiment in 2018.
- Improvements in stability and controls of measurement environment.
- Gas pressure dependence was studied.
- Fifth experiment in 2019.
- Test of mixture gas target.

Positron Coincidence

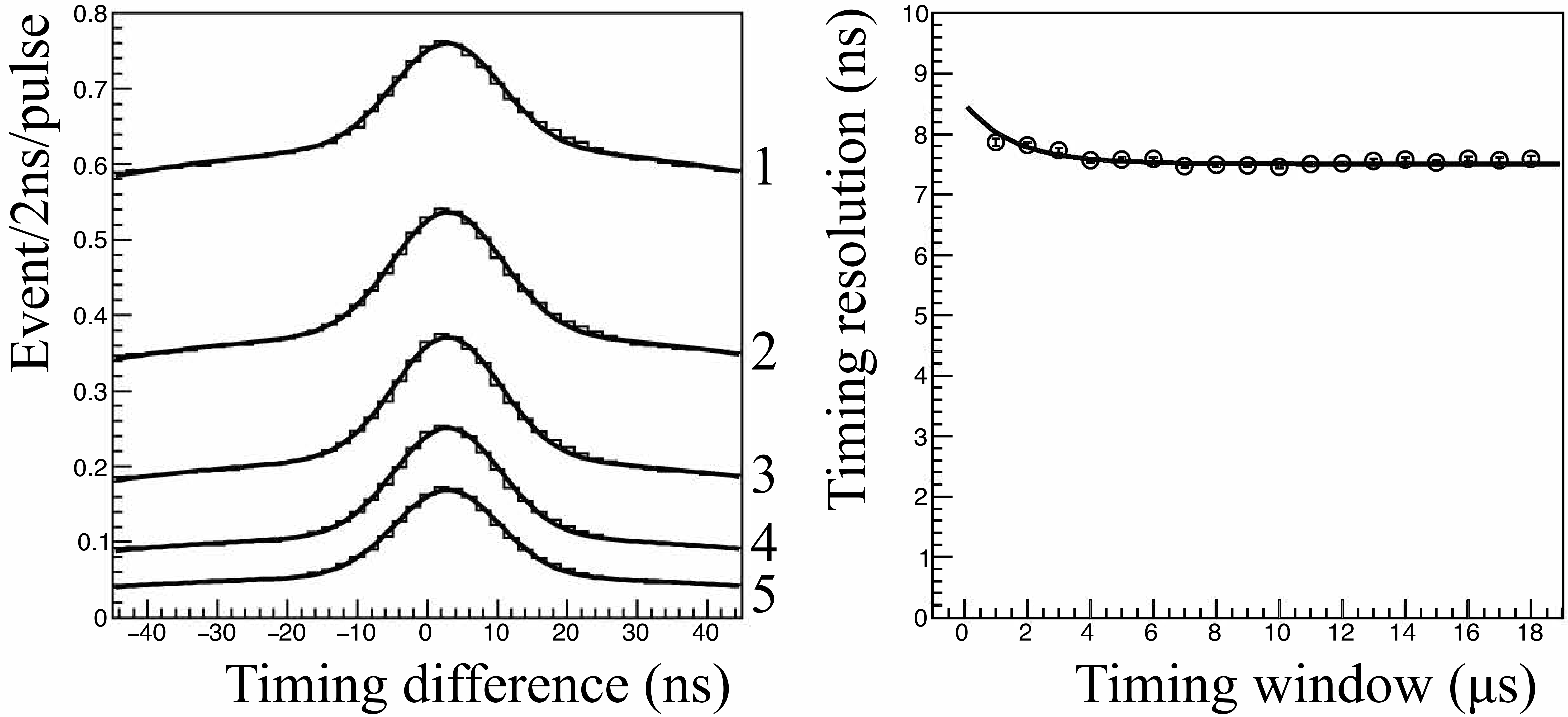

- (left) Time difference between hits on the near and far layers of the detector. The numbers on the right indicate the starting point of the 500 ns timing windows in µs. Curves are Gaussian on background.
- (right) Timing resolution of the detector, which is defined as 1σ of the Gaussian component of the timing difference.

Decay Positron Time Spectrum

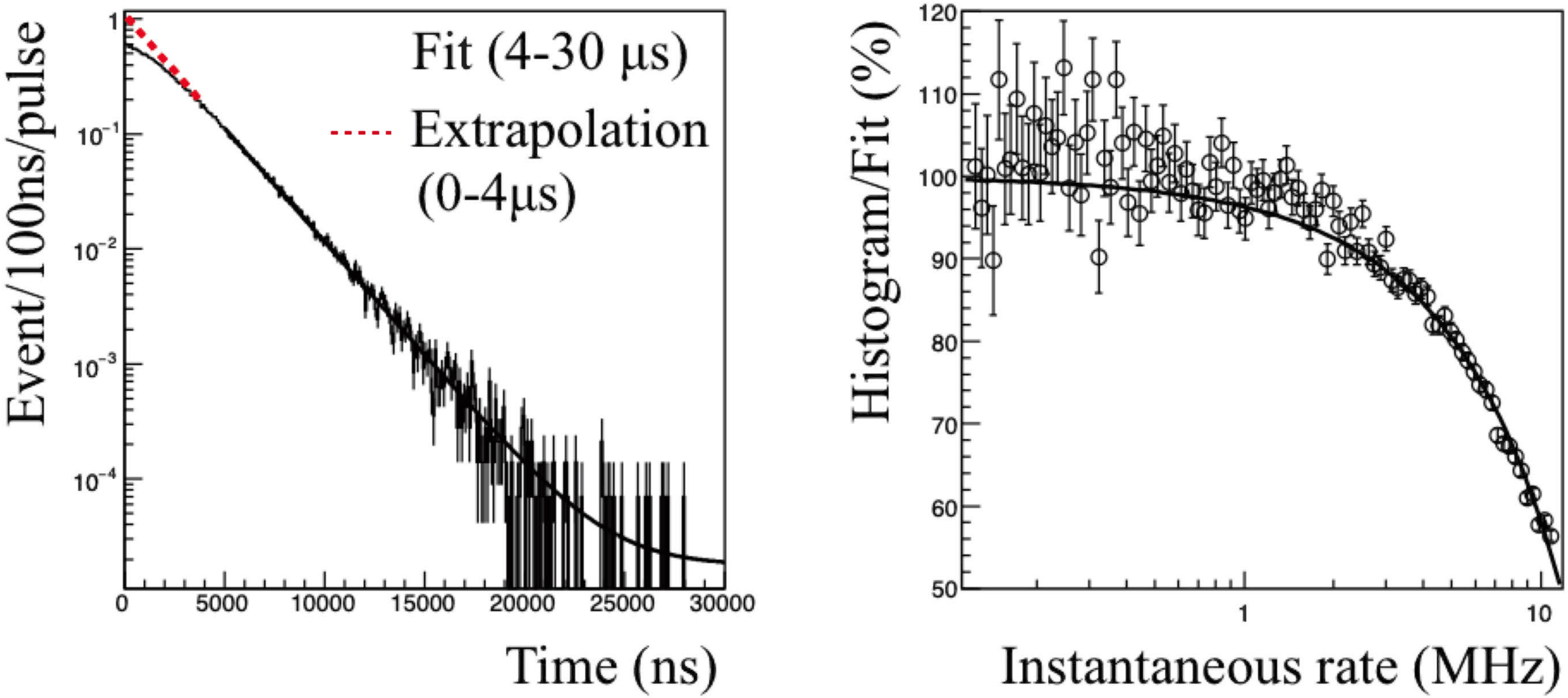

- (left) Time spectrum of decay positrons without microwave irradiation. The black solid curve corresponds to the fitting result with an exponential function on a constant background. The red dashed line indicates an extrapolation of the fitting function.
- (right) Pileup count loss as a function of the instantaneous event rate. The black curve indicates the fitting result with a model function.

Time Dependent Spin Flip Signal

- The Rabi oscillation was observed by taking the ratio of positron time spectra with and without microwave.
- Higher microwave power make the oscillation faster.
- Curves are theoretical expression the signal.
- The time integral of the oscillation gives the signal strength at a certain frequency of the resonance curve.

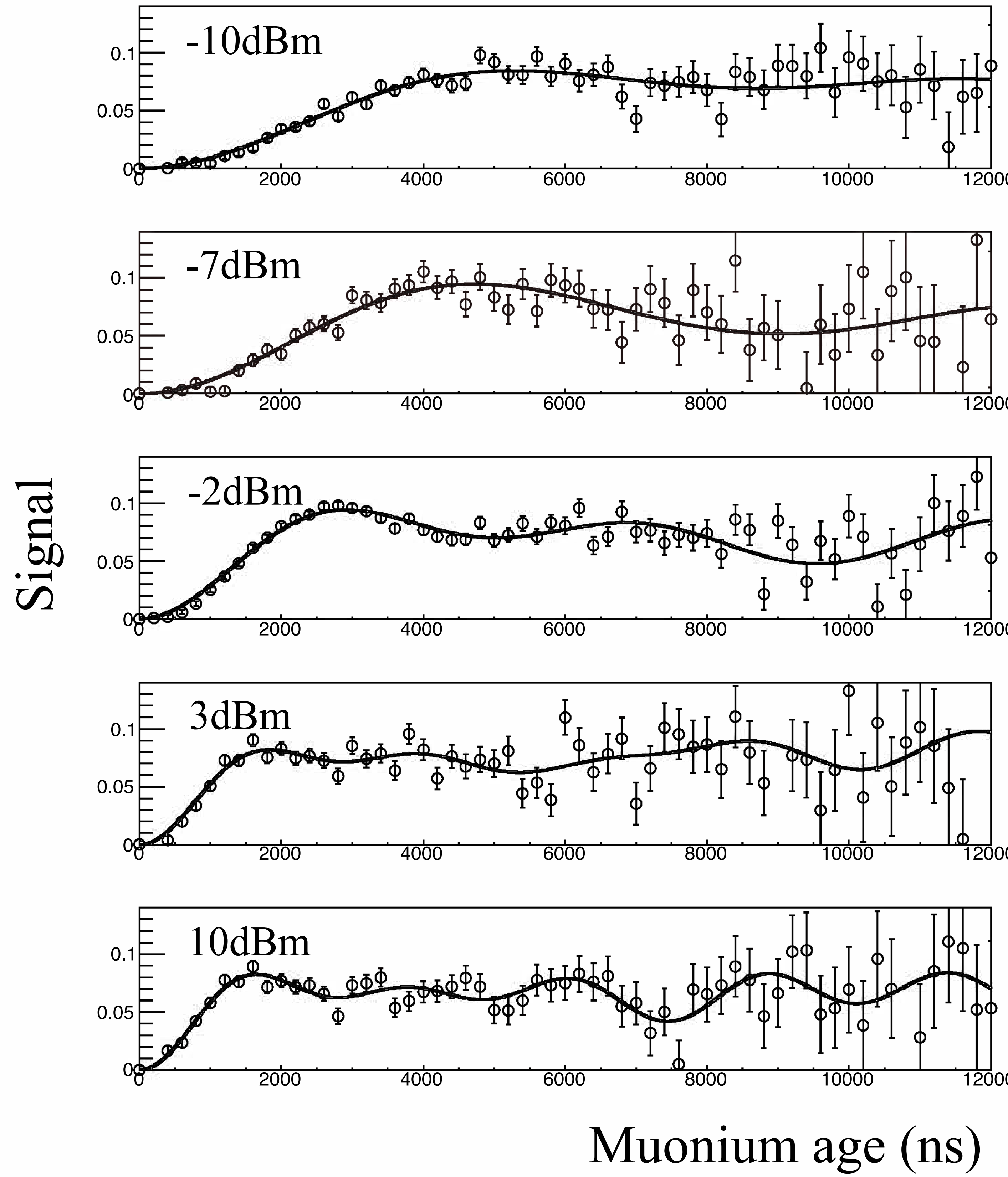

Resonance Lineshapes

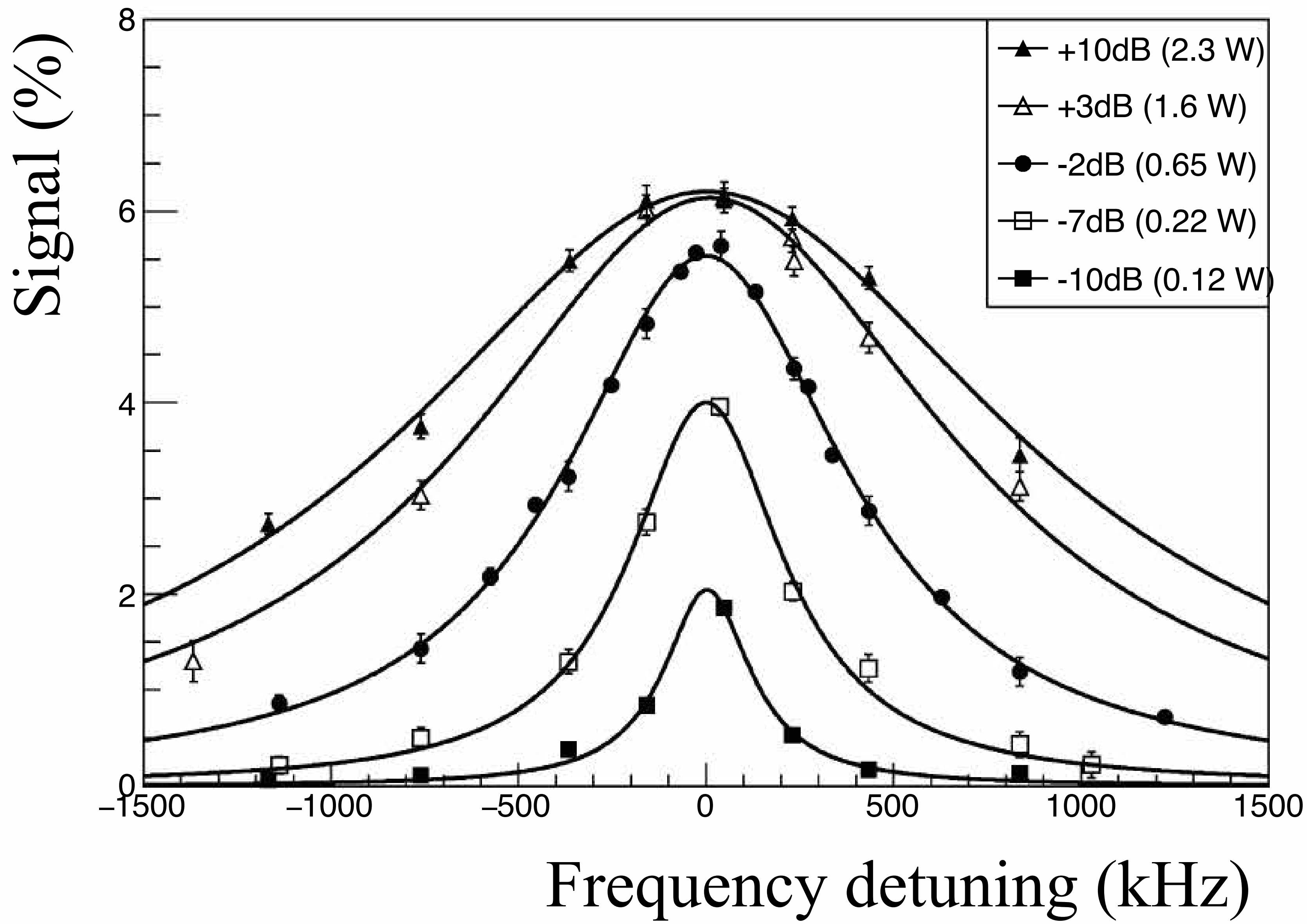

- Resonance lineshapes of the muonium HFS transition.
- The vertical axis shows the time integral of spin flip signal.
- The solid curves indicate to the fitting results with a Lorenz function.

Microwave Power Dependence

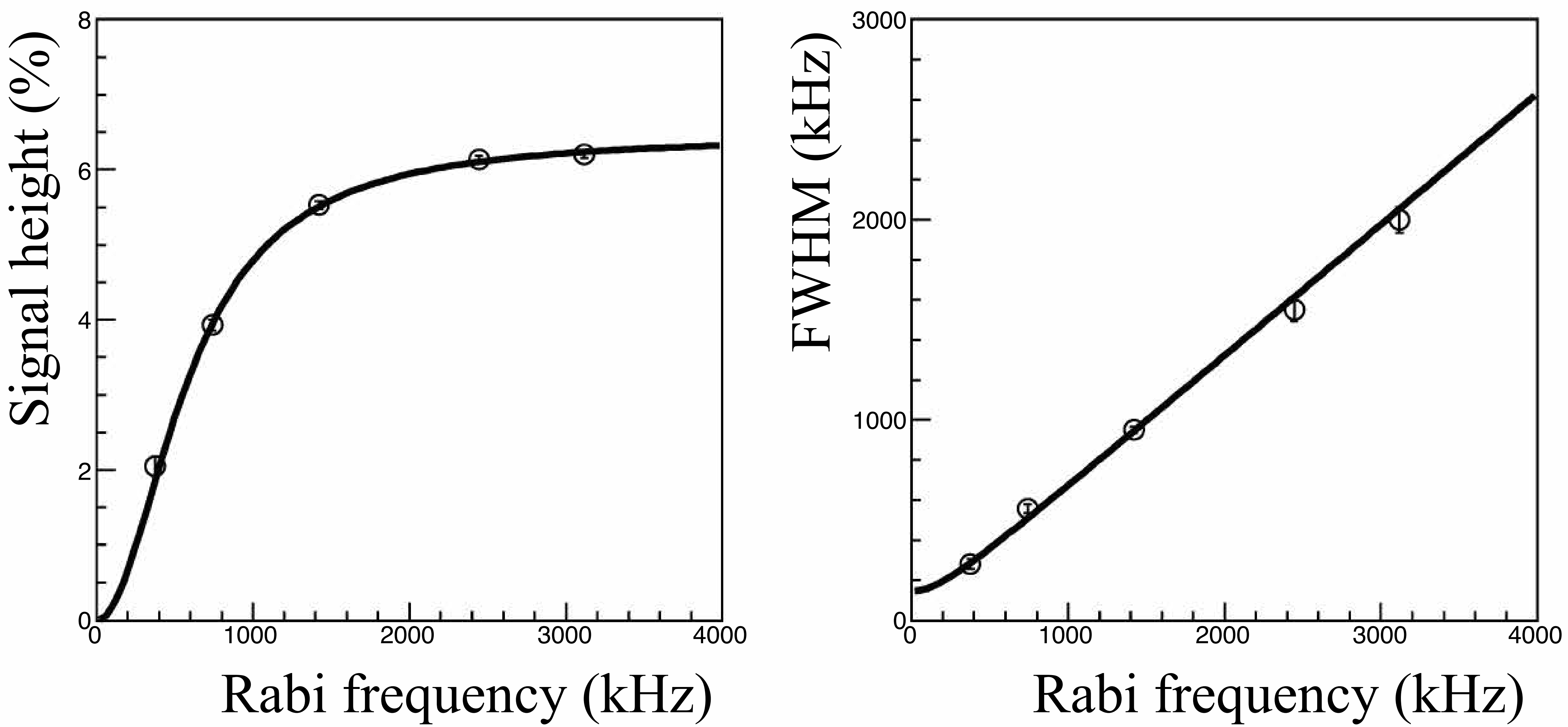

- Microwave power dependence of the resonance line- shape parameters: (a) the signal height; (b) the full-width- half-maximum (FWHM). Solid lines represent theoretical expressions.

Resonance Frequency

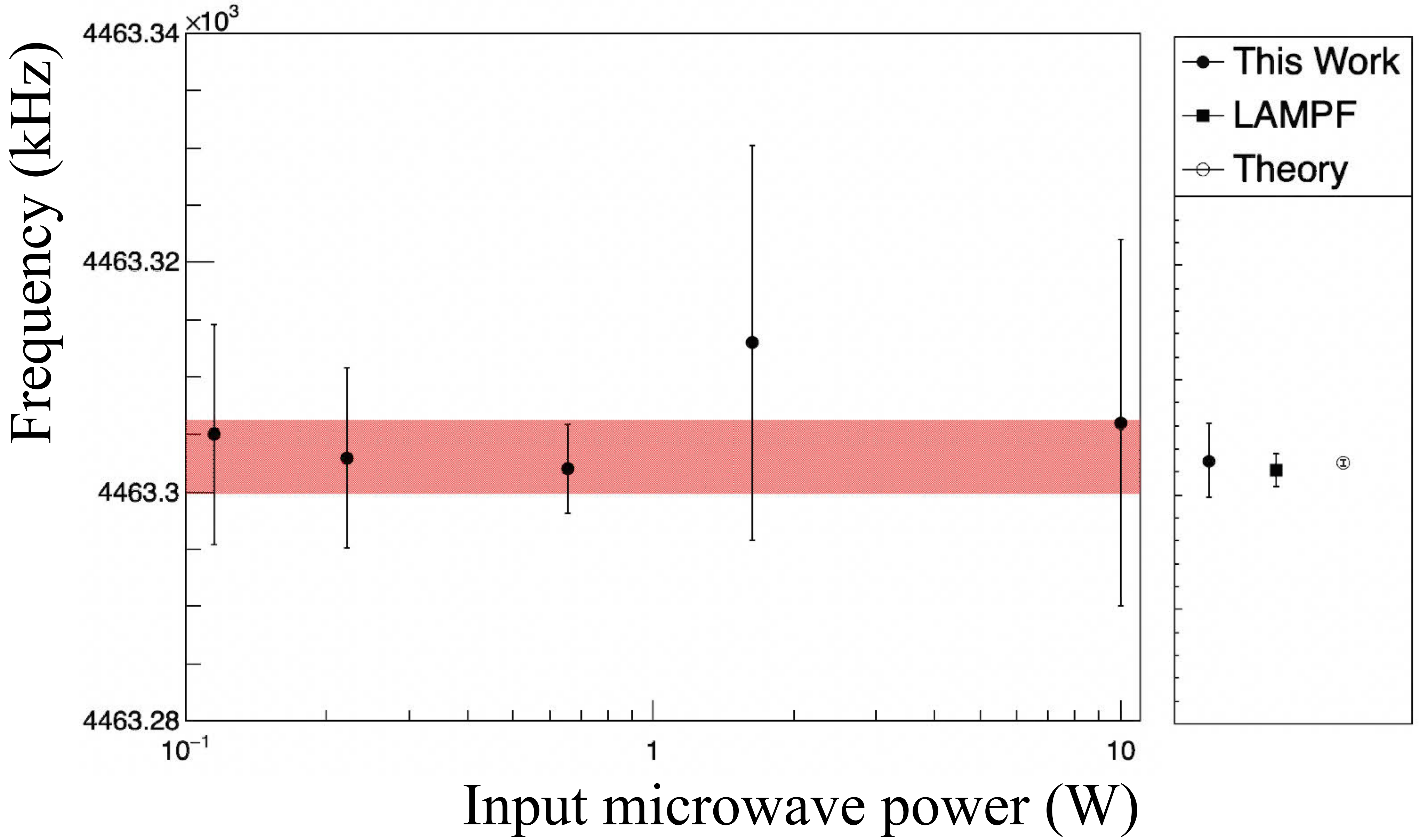

- (a) The muonium hyperfine transition frequency for several input microwave power settings. The red band shows the weighted average. (b) Comparison with the precursor experimental result and the theoretical prediction.

Microwave Power Optimization

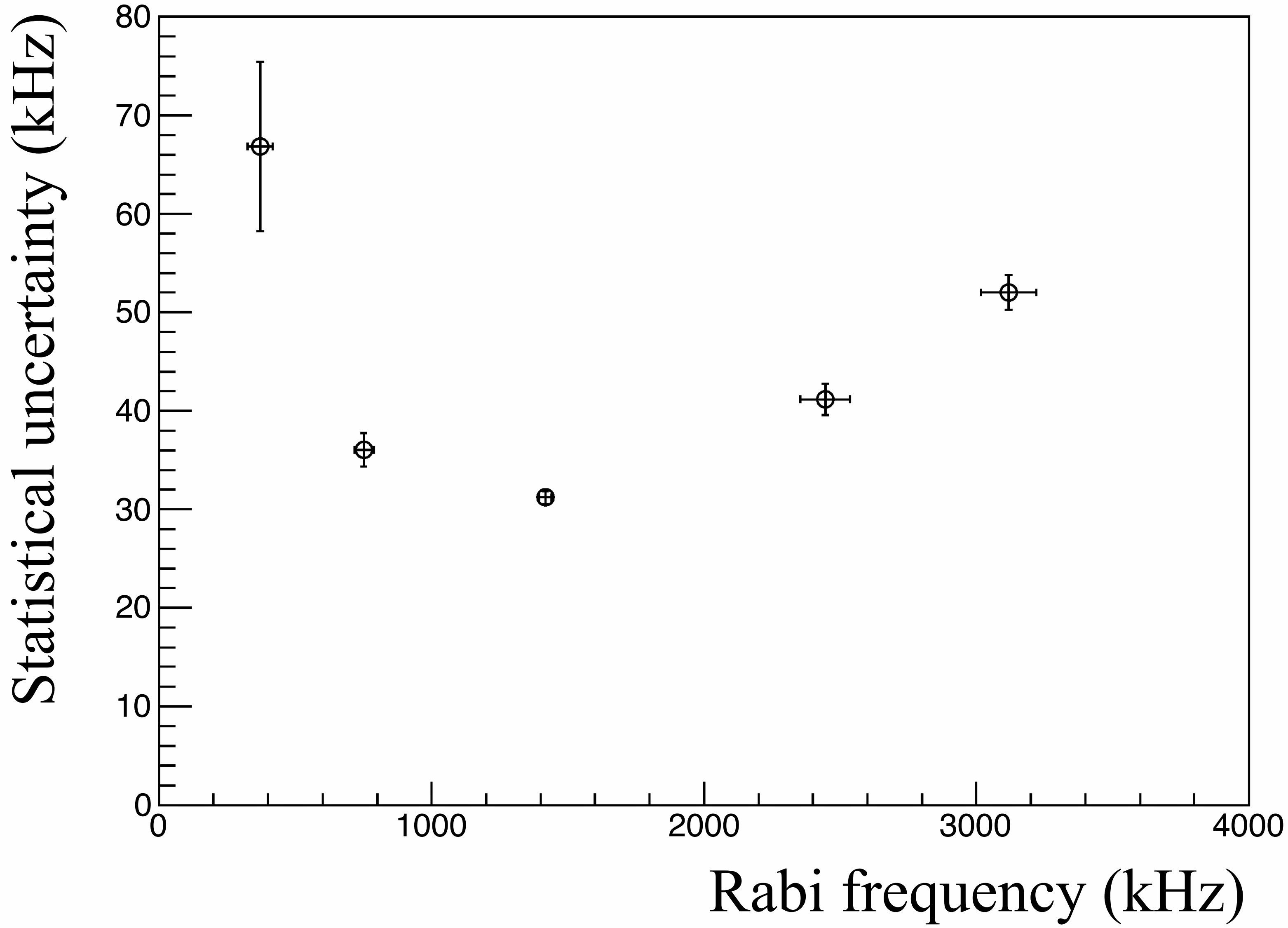

- Microwave power optimization.The ordinate indicates the statistical uncertainty in determining the resonance frequency. The positron statistics of $4{\times}10^8$ for each data point is assumed.

Systematic Uncertainty

Temporal variations
- Random fluctuation
- Drift in sequence

Microwave power

Muon beam intensity

Muon beam profile

Gas pressure drift (resonance shift)

Gas impurity effect (spin depolarization)

Static effects

Static magnetic field

Gas density zero-extrapolation (atomic collisional shift)

Detector pileup (rate dependent event loss)

Suppressed by taking the positron time spectra ratio

Atomic Collisional Shift

- **Resonance frequency shifts due to collisions with atoms in the target.**
- **The shift depends of the target pressure.**

$$\Delta\nu(p) = (1 + ap + bp^2)\Delta\nu(p=0)$$

$$a = 7.996(8) \times 10^{-6}/\text{bar (two-body)}$$

$$b = 5.5(1.1) \times 10^{-9}/\text{bar}^2 \text{ (three-body)}$$

- **For the case of krypton with the pressure of 1.0 atm, the resonance shifts -33 kHz.**
- **Systematic uncertainty due to pressure gauge accuracy is 46 Hz.**

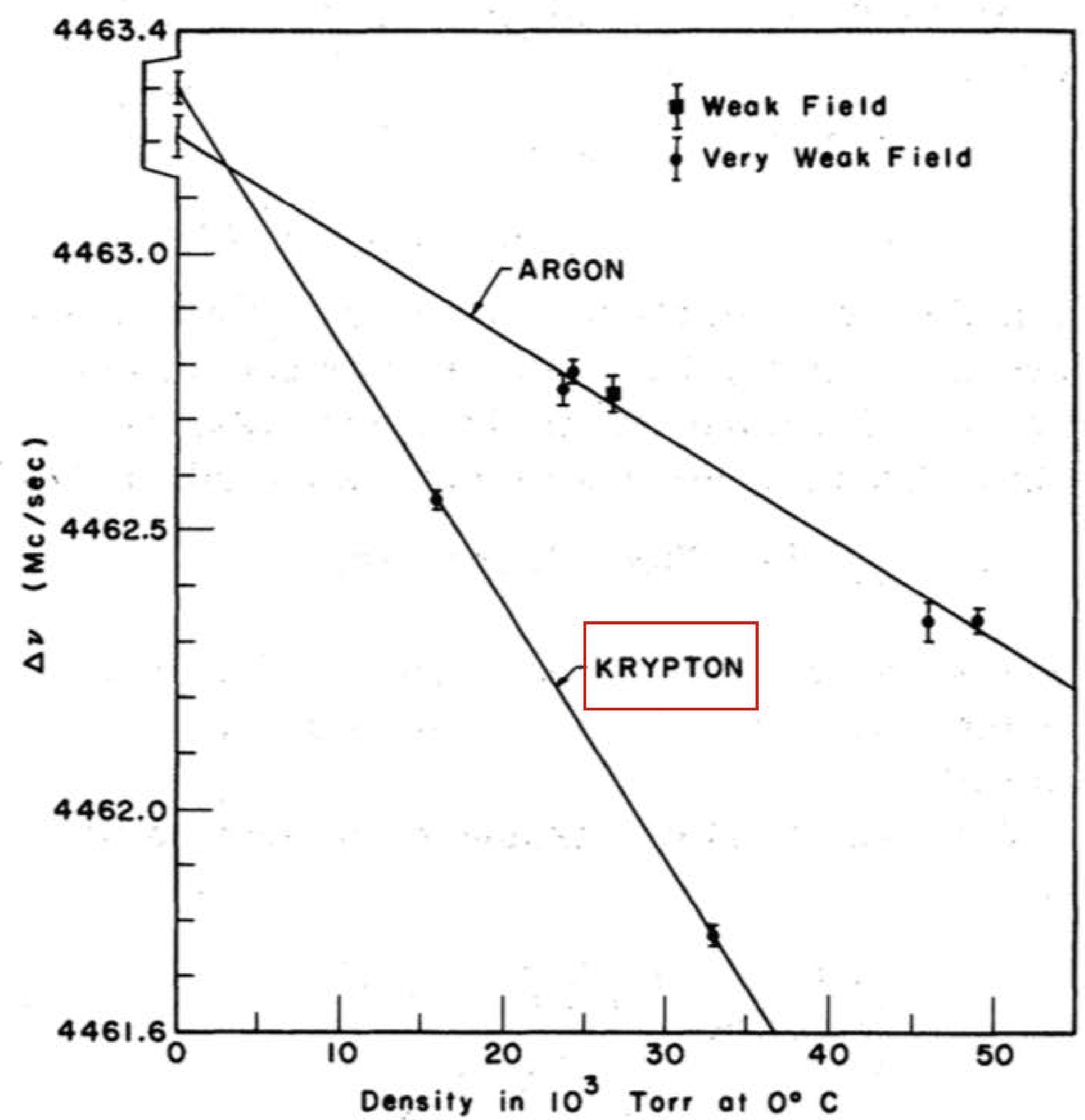

Values from D. E. Casperson *et al*., Phys. Lett. B, 59, 4 (1975).
Figure from P. A. Thompson *et al*., PRL, 22, 5, (1969).

Microwave Power Correction

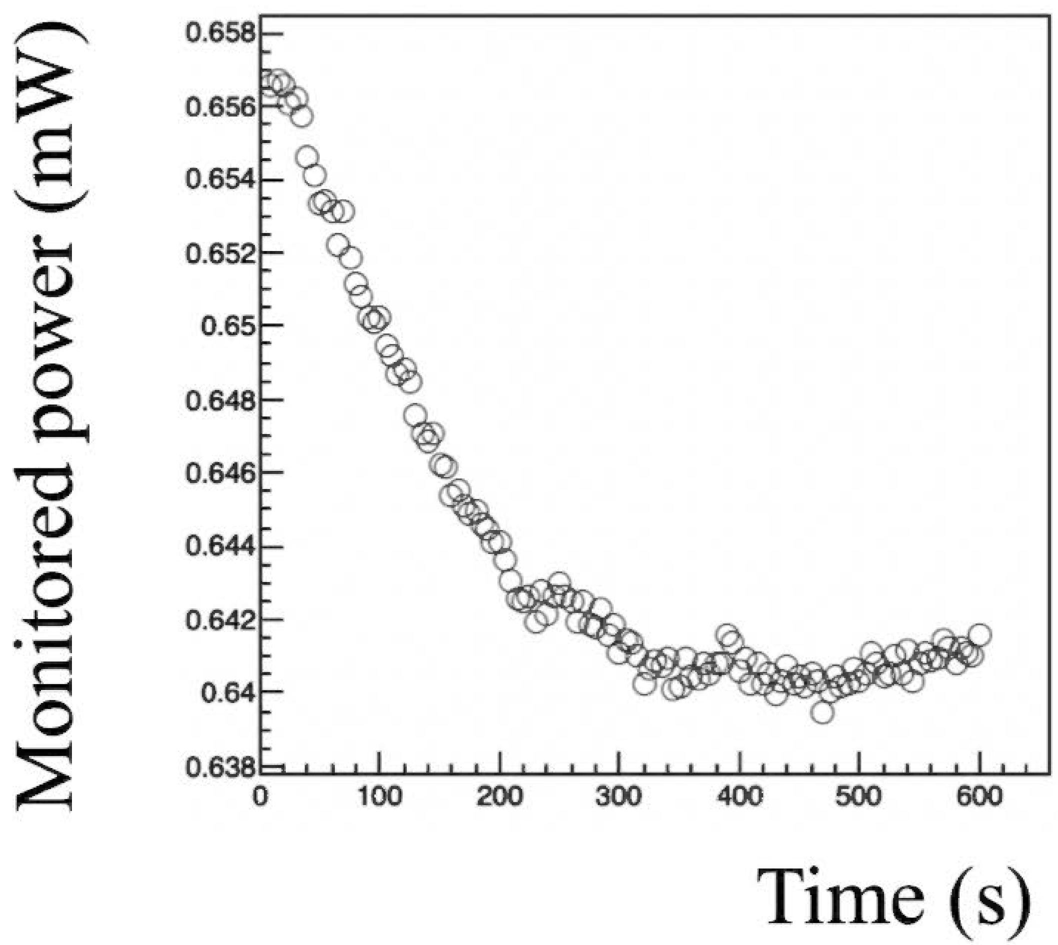

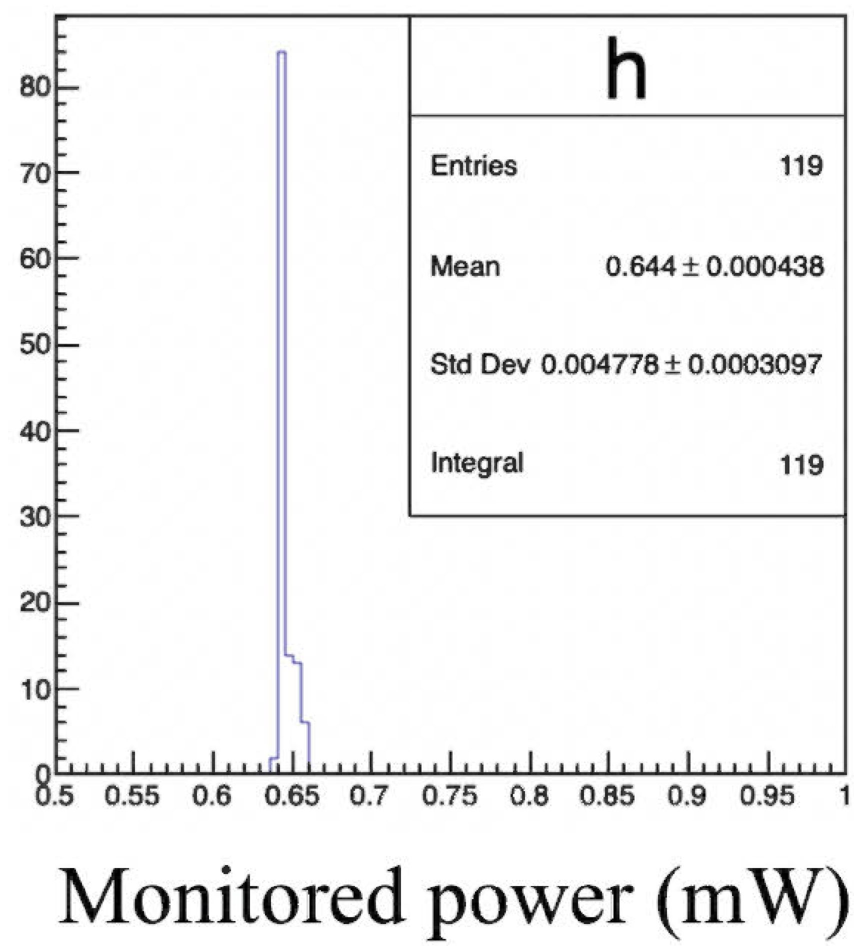

- Power correction was performed using the average value at each frequency data point.
- The systematic error is evaluated using the error in determining the average value.
- The uncertainty is estimated to be 37 Hz.

Detector Pileup

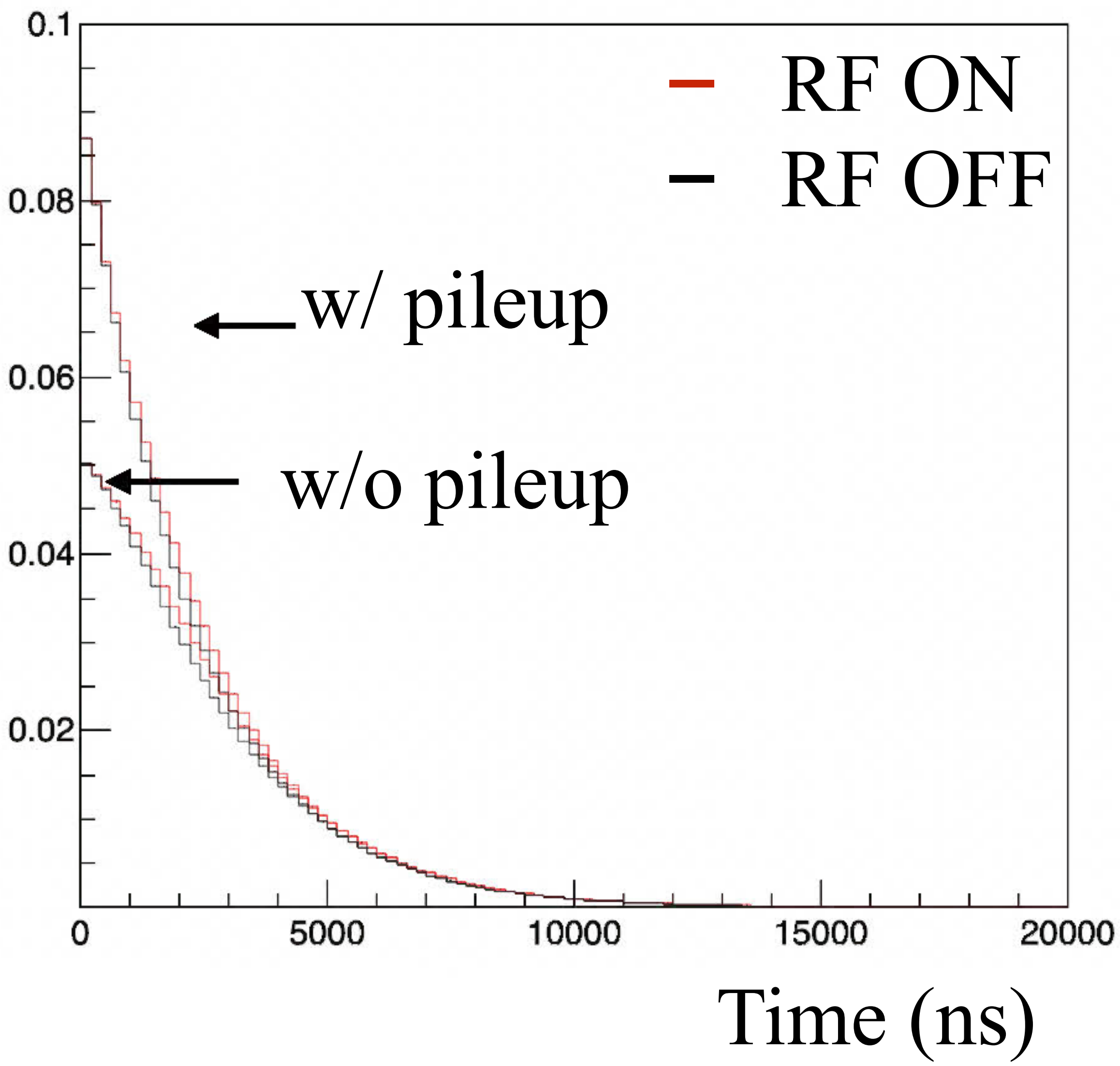

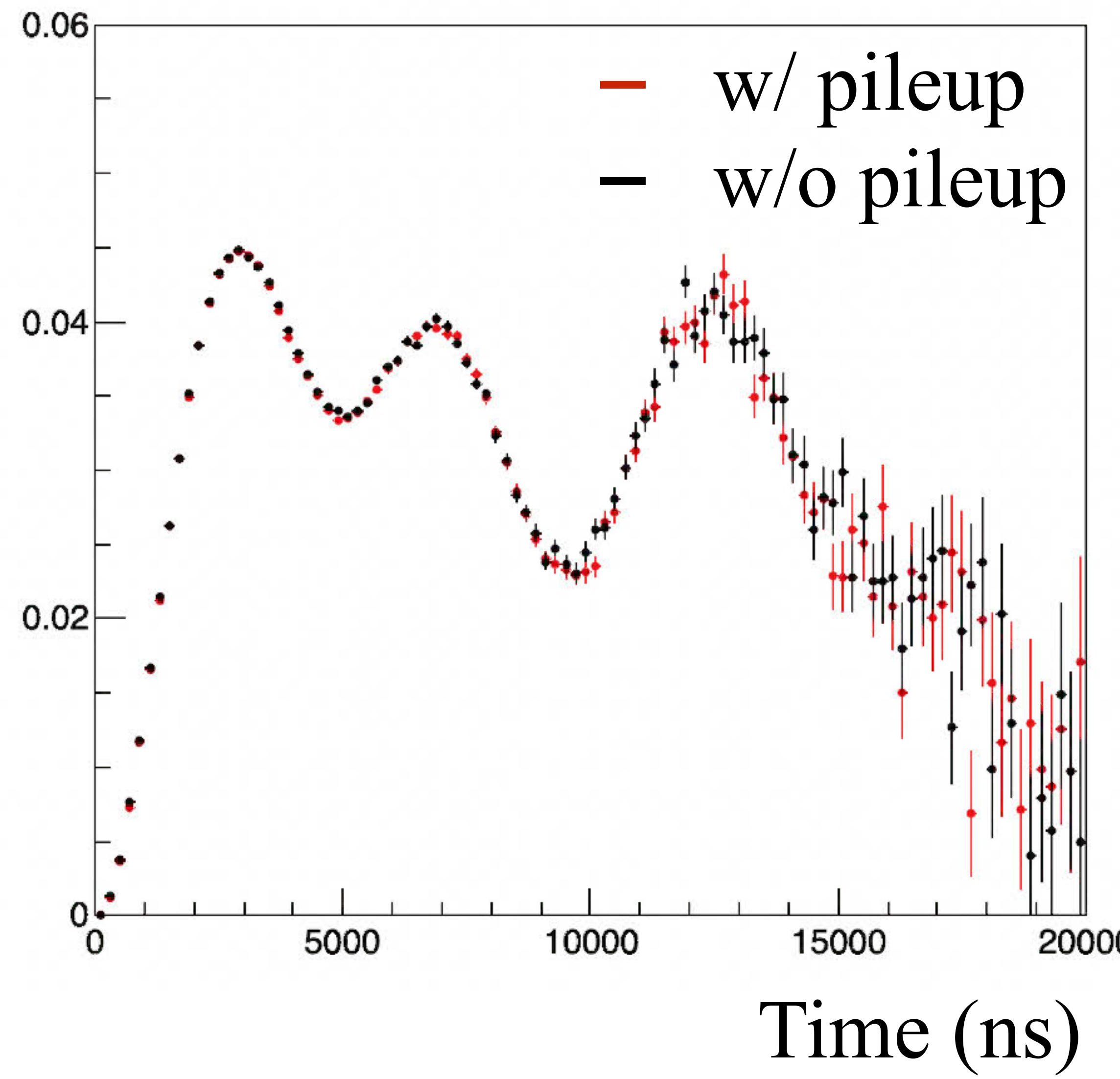

- Decay positron time spectra are simulated with and without microwave transition considering the pileup count loss.
- The time dependent signal is calculated with and without the pileup effect.
- Systematic uncertainty is estimated to be 19 Hz.

Static Magnetic Field

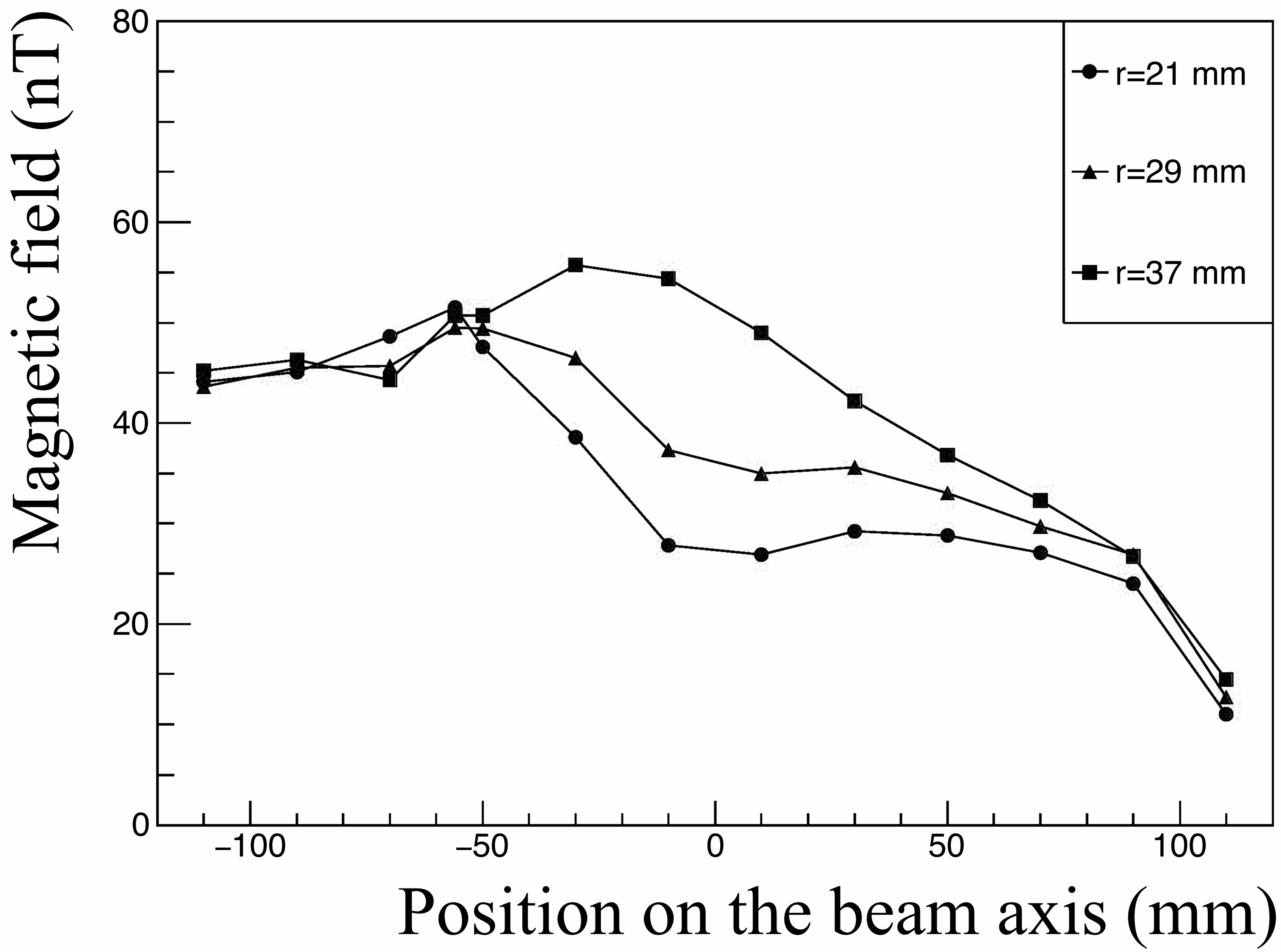

- Magnetic field strength on the longitudinal axis was measured by using the fluxgate probe.
- The Zeeman shifts of muonium levels are calculated.
- Systematic uncertainty is negligibly small.

Summary of Systematics

Source	Contribution (Hz)
Atomic collisional shift	46
Microwave power	37
Detector pileup	19
Static magnetic field	0
Gas pressure fluctuation	6
Gas impurity buildup	12
Muon beam intensity	0
Muon beam profile	0
Total	63

- Currently, the systematic uncertainties are sufficiently small compared to the statistical uncertainty.
- However, after completion of the new beam line, statistical precision is significantly improved and it is more important to understand and suppress systematic uncertainties.
- A pressure gauge with better accuracy, microwave power switching, water cooling of the cavity will help improvements.

Upgrades in Progress and Implemented

- Larger microwave cavity which resonates in TM220 mode
  - Y.Ueno (RIKEN).
- Microwave switching
  - T. Tanaka (U. Tokyo)
- Krypton-Helium mixture gas target to offset the atomic collisional shift
  - S.Seo (U. Tokyo).
- Detailed analysis of the time-dependent spin flip signal.
  - S.Nishimura (U. Tokyo)

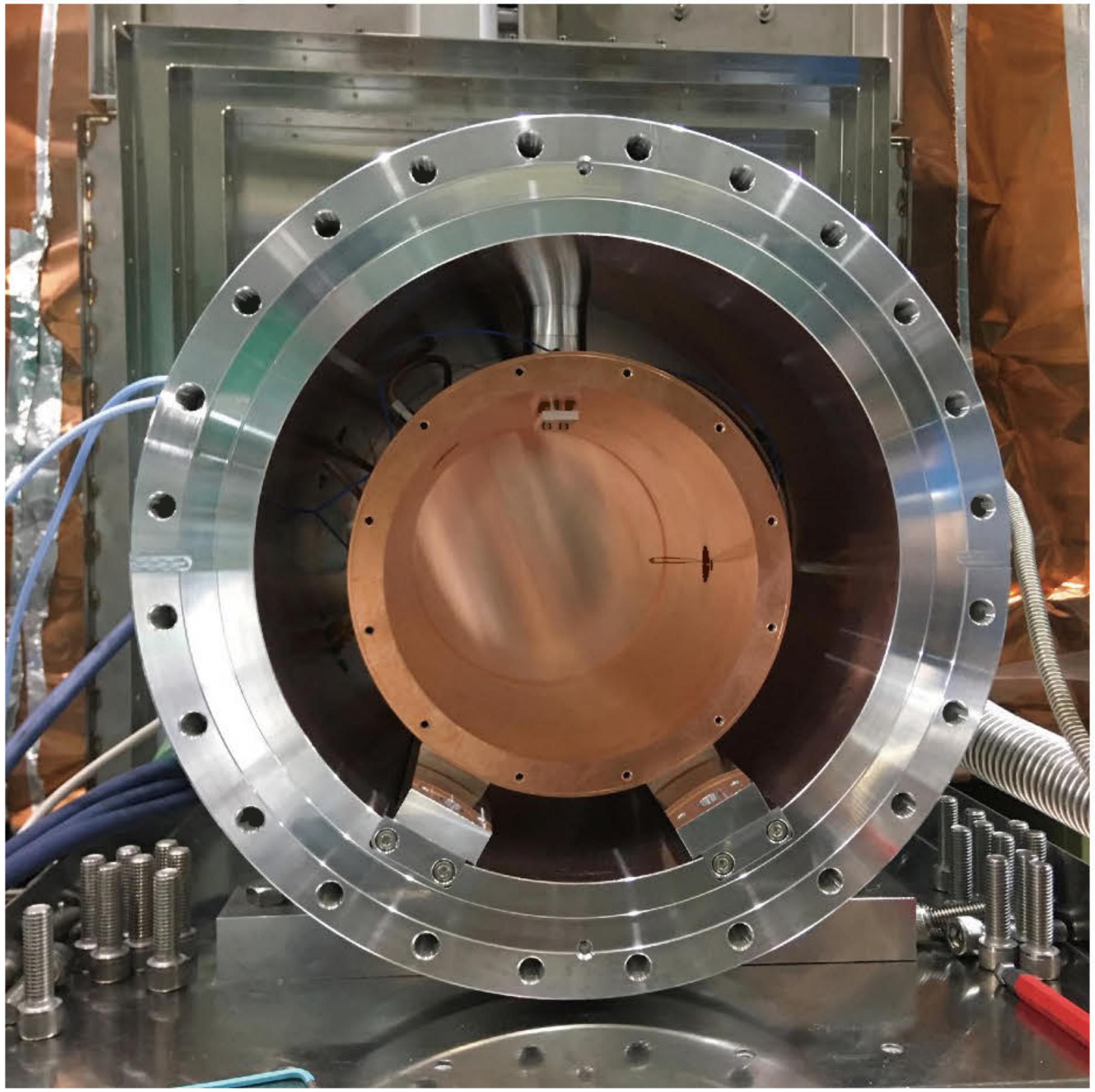

Toward High-field Experiment

- The new beam line at the 1st experimental hall in MLF with larger solid angle is under construction.
- The superconducting magnet for high-field measurement was delivered at J-PARC.
- Passive shimming method for field uniformity was developed.
- NMR probe for field measurement is under development.

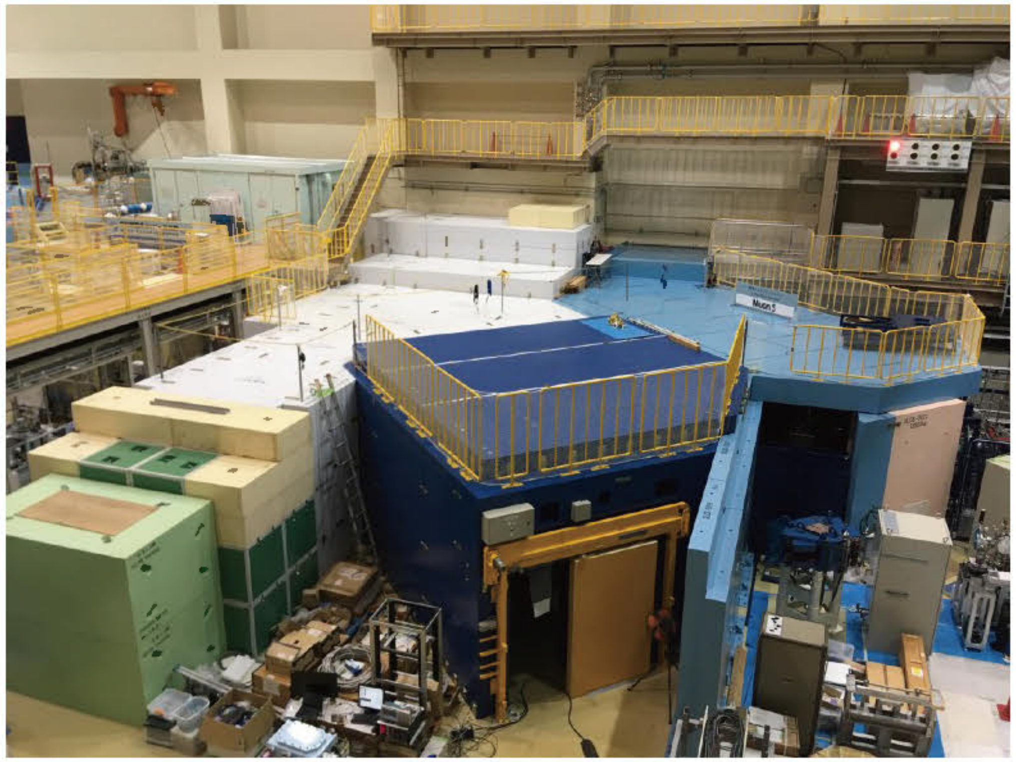

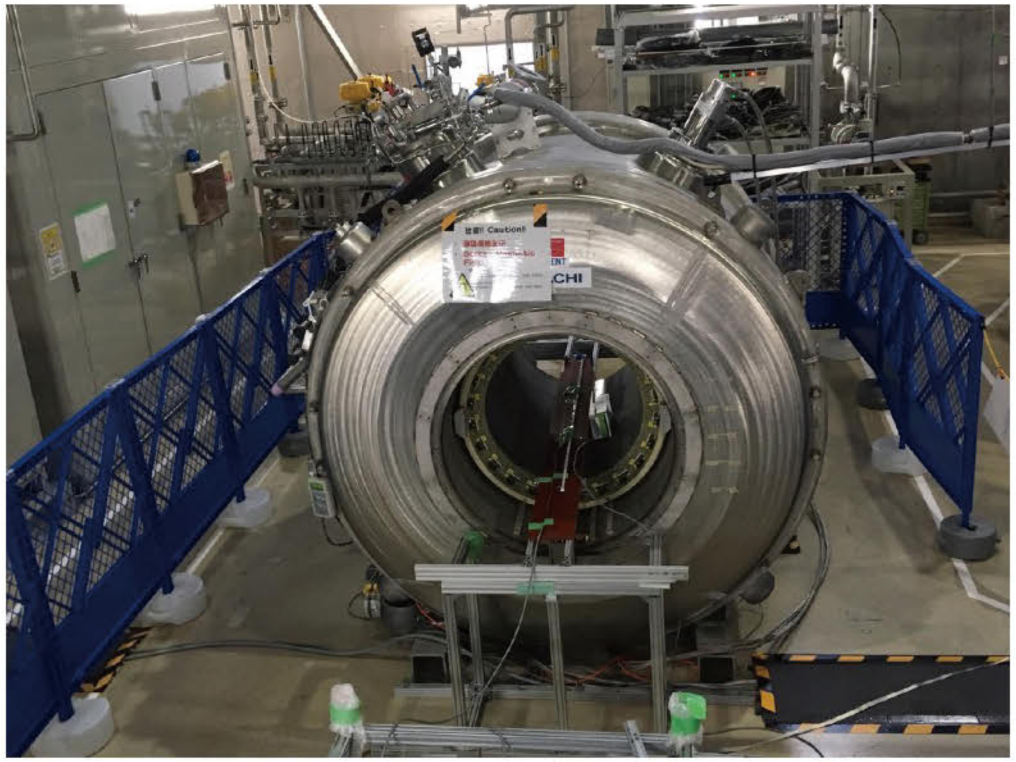

Future Dreams

- Improvement in the positron detector and precise control of a magnetic field enable:
  - High precision measurement of the mean lifetime of muonium.
  - A search for axion-like particle by field sweep measurement.
  - Precision measurement of the bound-state g-factor.
- Muonium emission into vacuum from silica aerogel.
  - Atomic-collision-free measurement in vacuum.
- Direct measurement of the hyperfine transition without a microwave field using FFT analysis.
  - Free from field-related systematics.
- Laser cooling of muonium.
  - Bose-Einstein condensation of muonium.
- Highest intensity pulsed muon beam and advanced instrumentation unveil unexplored areas in muon physics.

Summary

- The ground-state hyperfine splitting in muonium atom is an ideal observable to test bound-state QED theory.
- MuSEUM collaboration aims to improve a measurement precision of the muonium HFS by a factor of ten.
- The high-intensity pulsed muon beam and high-rate capable positron detector enable us to realize a new experiment at J-PARC.
- The first observation of muonium HFS resonance was reported after the experiment in 2016. The principle is proofed.
- Improved experiment was conducted in 2017 after upgrades and the result is comparable to the precursor experimental one.
- Further improvements are under study.